

Crystalline evolutions with rapidly oscillating forcing terms

ANDREA BRAIDES, ANNALISA MALUSA AND MATTEO NOVAGA

Abstract. We consider the evolution by crystalline curvature of a planar set in a stratified medium, modeled by a periodic forcing term. We characterize the limit evolution law as the period of the oscillations tends to zero. Even if the model is very simple, the limit evolution problem is quite rich, and we discuss some properties such as uniqueness, comparison principle and pinning/depinning phenomena.

Mathematics Subject Classification (2010): 53C44 (primary); 35B27 (secondary).

1. Introduction

In this paper we are interested in the asymptotic behavior of motions of planar curves according to the law

$$v = \kappa_\varphi + g\left(\frac{x}{\varepsilon}\right), \quad (1.1)$$

where v is the normal velocity, κ_φ is the crystalline square curvature (see Definition 2.1 for precise definitions), $g : \mathbb{R} \rightarrow \mathbb{R}$ is a forcing term depending only on the horizontal variable x , and $\varepsilon > 0$ is a small parameter modeling the rapidly oscillating medium where the curve evolves. For simplicity, we shall assume that g is 1-periodic and takes only two values $\alpha < 0 < \beta$, with average $\frac{\alpha+\beta}{2}$.

Crystalline evolutions play an important role in many models of phase transitions and Materials Science (see [28, 33] and references therein) and have been significantly studied in recent years (see for instance [1, 6, 7, 23, 25]). The term $g\left(\frac{x}{\varepsilon}\right)$ models a heterogeneous layered medium, which we assume periodic exactly in one of the direction orthogonal to the Wulff shape of the crystalline perimeter (in our case, for simplicity, the x -direction). Our aim is understanding the effect of the oscillations in the asymptotic limit $\varepsilon \rightarrow 0$, which is a typical homogenization problem.

We will show that, at scale ε , the curves may undergo a microscopic “facet breaking” phenomenon, with small segments of length proportional to ε being created and reabsorbed. After dealing with this aspect, we show that the motion of a limit of curves satisfying (1.1) can be characterized by different laws of motion in the x and y -directions: the portions of the curve moving in the vertical direction travel with a velocity equal to $\kappa_\varphi + \frac{\alpha+\beta}{2}$, whereas the portions moving in the horizontal direction are either pinned or travel with velocity equal to $\langle \kappa_\varphi + g \rangle$, where $\langle \cdot \rangle$ denotes the harmonic mean (see Theorem 4.6). Note that such law does not correspond to a forced crystalline evolution.

Our analysis can be set in a large class of variational evolution problems dealing with limits of motions driven by functionals F_ε depending on a small parameter [10]. In some cases, the limit motion can be directly related to the Γ -limit of F_ε (see, e.g., [12, 14, 20, 32]), but in general this is not the case. For oscillating functionals, the energy landscape of the energies F_ε can be quite different from that of their Γ -limit and the related motions can be influenced by the presence of local minima which may give rise to “pinning” phenomena (motions may be attracted by those local minima) or to effective homogenized velocities [13, 31]. In the case of geometric motions, a general understanding of the effects of microstructure is still missing. Recently, some results have been obtained for (two-dimensional) crystalline energies, for which a simpler description can be sometimes given in terms of a system of ODEs. Such results include discrete approximations of crystalline energies, which can be understood as a simple way to introduce a periodic dependence, corresponding to that of an underlying square lattice [11, 13, 15, 16]. Such discrete energies correspond to continuum inhomogeneous perimeter energies of the form

$$F_\varepsilon(E) = \int_{\partial E} a\left(\frac{x}{\varepsilon}, \frac{y}{\varepsilon}\right) (|v_1^E| + |v_2^E|) d\mathcal{H}^1, \quad E \subset \mathbb{R}^2,$$

converging to the square perimeter in the sense of Γ -convergence [3, 9], and the corresponding geometric motions can be studied using the minimizing-movement approach introduced by Almgren, Taylor and Wang [2]. The suitably defined limit motions [10] correspond to modified crystalline flows.

In our case, equation (1.1) corresponds to the L^2 -gradient flow for the energy functional

$$F_\varepsilon(E) = \int_{\partial E} (|v_1^E| + |v_2^E|) d\mathcal{H}^1 + \int_E g\left(\frac{x}{\varepsilon}\right) d\mathcal{L}^2, \quad E \subset \mathbb{R}^2,$$

where we identify the evolving curve with the boundary of a set E . Note that, since the volume term converges to $\frac{\alpha+\beta}{2}\mathcal{L}^2(E)$, the (Γ) -limit as $\varepsilon \rightarrow 0$ of the functionals F_ε is the functional

$$\overline{F}(E) = \int_{\partial E} (|v_1^E| + |v_2^E|) d\mathcal{H}^1 + \frac{\alpha+\beta}{2}\mathcal{L}^2(E).$$

As a consequence of our analysis, it turns out that the asymptotic behavior as $\varepsilon \rightarrow 0$ of the evolutions corresponding to (1.1) does not coincide with the gradient flow of

\overline{F} , which is $v = \kappa_\varphi + \frac{\alpha+\beta}{2}$. Even in the case $\alpha + \beta = 0$ the limit motion cannot be derived as a gradient flow of a modified (crystalline) perimeter.

A similar result for g modeling a periodic chessboard-like structure can be found in [29]. Note that, if the crystalline curvature is replaced by the usual curvature and the initial curve is a graph in the y -direction, the homogenization problem corresponding to (1.1) has been studied in [18], where it is proved that the limit evolution law is indeed the curvature flow with a constant forcing term. We also mention that an analysis of the asymptotic behavior of the semilinear problem

$$u_t = u_{xx} + g\left(\frac{u}{\varepsilon}\right),$$

can be found in [17]. That problem has some features in common with our geometric evolution, since it can be seen as the linearization of the isotropic version of (1.1).

The plan of the paper is the following: in Section 2 we introduce the notion of crystalline curvature and the evolution problem we want to study. In Section 3 we introduce the notion of calibrable edge, that is, an edge of the curve which does not break during the evolution, and we characterize the calibrability of an edge in terms of its length and of the position of its endpoints. Finally, in Section 4 we characterize the limit evolution law as $\varepsilon \rightarrow 0$ first for rectangular sets, then for polyrectangles, and eventually for more general sets, including bounded convex sets.

2. Setting of the problem

2.1. Notation

Given $\xi, \eta \in \mathbb{R}^2$, we denote by $\xi \cdot \eta$ the usual scalar product between ξ and η and by $]\xi, \eta[$ (respectively, $[\xi, \eta]$) the open (respectively, closed) segment joining ξ and η . The canonical basis of \mathbb{R}^2 will be denoted by $e_1 = (1, 0)$, $e_2 = (0, 1)$.

The 1-dimensional Hausdorff measure and the 2-dimensional Lebesgue measure in \mathbb{R}^2 will be denoted by \mathcal{H}^1 and \mathcal{L}^2 , respectively.

We say that a set $E \subseteq \mathbb{R}^2$ is a *Lipschitz set* if E is open and ∂E can be written, locally, as the graph of a Lipschitz function (with respect to a suitable orthogonal coordinate system). The *outward normal* to ∂E at ξ , that exists \mathcal{H}^1 -almost everywhere on ∂E , will be denoted by $\nu^E(\xi) = (\nu_1^E, \nu_2^E)$.

The Hausdorff distance between the two sets $E, F \in \mathbb{R}^2$ will be denoted by $d_H(E, F)$.

2.2. The crystalline square curvature

We briefly recall how to give a notion of mean curvature κ^E which is consistent with the requirement that a geometric evolution $E(t)$ that reduces as fast as possible the

energy functional

$$P(E) = \int_{\partial E} (|v_1^E| + |v_2^E|) d\mathcal{H}^1$$

has normal velocity $\kappa^{E(t)}$ \mathcal{H}^1 -almost everywhere on $\partial E(t)$.

The functional $P(E)$ is the perimeter associated to the norm $\varphi(x, y) = \max\{|x|, |y|\}$, $(x, y) \in \mathbb{R}^2$; that is, the Minkowski content derived by considering (\mathbb{R}^2, φ) as a normed space. The density $\varphi^\circ(x, y) = |x| + |y|$ is the *polar function* of φ , defined by $\varphi^\circ(\xi^\circ) := \sup\{\xi \cdot \xi^\circ, \varphi(\xi) \leq 1\}$.

The Wulff shape $\mathcal{W} = \{\varphi(\xi) \leq 1\}$ and the Frank diagram $\mathcal{F} = \{\varphi^\circ(\xi) \leq 1\}$ are the square $K = [-1, 1]^2$ and the square with corners at $(\pm 1, 0)$ and $(0, \pm 1)$, respectively.

Given a nonempty compact set $E \subseteq \mathbb{R}^2$, we denote by d_φ^E the *oriented φ -distance function* to ∂E negative inside E ; that is,

$$d_\varphi^E(\xi) = \inf_{\eta \in E} \varphi(\xi - \eta) - \inf_{\eta \notin E} \varphi(\xi - \eta), \quad \xi \in \mathbb{R}^2.$$

The function d_φ^E is Lipschitz, $\varphi^\circ(\nabla d_\varphi^E(\xi)) = 1$ at each its differentiability point ξ , and

$$\nabla d_\varphi^E(\xi) = \frac{v_E(\xi)}{\varphi^\circ(v_E(\xi))}$$

at every $\xi \in \partial E$ where v_E is well defined.

Since \mathcal{W}_φ is neither smooth nor strictly convex, the intrinsic normal direction to ∂E is not uniquely determined, in general, even if the set E is smooth. It is known that the normal cone at $\xi \in \partial E$ is well defined whenever ξ is a differentiability point for d_φ^E and it is given by $T_{\varphi^\circ}(\nabla d_\varphi^E(\xi))$, where

$$T_{\varphi^\circ}(\xi^\circ) := \left\{ \xi \in \mathbb{R}^2, \xi \cdot \xi^\circ = (\varphi^\circ(\xi))^2 \right\}, \quad \xi^\circ \in \mathbb{R}^2.$$

If $\varphi^\circ(\xi^\circ) = 1$, a direct computation gives

$$T_{\varphi^\circ}(\xi^\circ) = \begin{cases} (1, 1) & \xi^\circ \in \llbracket e_1, e_2 \rrbracket \\ (1, -1) & \xi^\circ \in \llbracket e_1, -e_2 \rrbracket \\ (-1, -1) & \xi^\circ \in \llbracket e_2, -e_1 \rrbracket \\ (-1, 1) & \xi^\circ \in \llbracket -e_2, -e_1 \rrbracket \end{cases} \begin{cases} T_{\varphi^\circ}(e_1) = \llbracket (1, 1), (1, -1) \rrbracket \\ T_{\varphi^\circ}(e_2) = \llbracket (-1, 1), (1, 1) \rrbracket \\ T_{\varphi^\circ}(-e_1) = \llbracket (-1, 1), (-1, -1) \rrbracket \\ T_{\varphi^\circ}(-e_2) = \llbracket (-1, -1), (1, -1) \rrbracket \end{cases} \quad (2.1)$$

(see Figure 2.1).

The notion of intrinsic curvature in (\mathbb{R}^2, φ) is based on the existence of regular selections of $T_{\varphi^\circ}(\nabla d_\varphi^E)$ on ∂E .

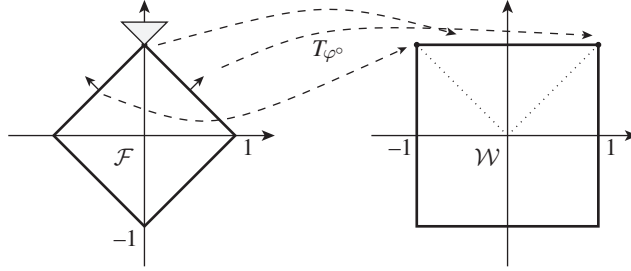


Figure 2.1. The square crystalline norm φ and the map T_{φ° .

Definition 2.1 (φ -regular set, Cahn-Hoffmann field, mean φ -curvature). We say that an open set $E \subseteq \mathbb{R}^2$ is φ -regular if ∂E is a compact Lipschitz curve and there exists a vector field $n_\varphi \in \text{Lip}(\partial E; \mathbb{R}^2)$ such that $n_\varphi \in T_{\varphi^\circ}(\nabla d_\varphi^E) \mathcal{H}^1$ -almost everywhere on ∂E .

Any such selection of the multivalued function $T_{\varphi^\circ}(\nabla d_\varphi^E)$ on ∂E is called a *Cahn-Hoffmann vector field* for ∂E associated to φ , and $\kappa_\varphi = \text{div } n_\varphi$ is the related *mean φ -curvature* (*crystalline square mean curvature*) of ∂E . Pictures of a φ -regular and a non- φ -regular set are included in Figure 2.2.

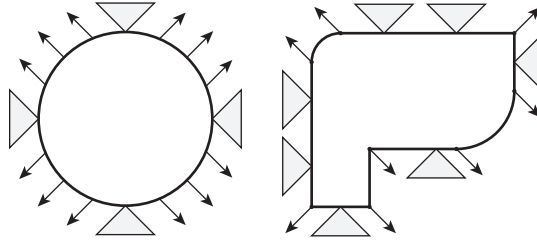


Figure 2.2. A non φ -regular set (left) and a φ -regular set (right).

Remark 2.2. Note that, unlike the outer (euclidean) unit normal ν^E , a Cahn-Hoffmann field is defined everywhere on ∂E .

Remark 2.3. Any Cahn-Hoffmann vector field n_φ has gradient orthogonal to the normal direction, so that $\text{div } n_\varphi$ equals the tangential divergence of the field.

2.3. Forced crystalline curvature flow

The appropriate way of describing a geometric evolution $E(t)$, starting from a given φ -regular set E and trying to reduce as fast as possible the energy functional

$$F(E(t)) = P_\varphi(E(t)) + V(E(t)) = \int_{\partial E(t)} (|\nu_1^E(t)| + |\nu_2^E(t)|) d\mathcal{H}^1 + \int_{E(t)} f d\mathcal{L}^2,$$

is a suitable weak version of the law

$$v = \kappa_\varphi + f, \quad \text{on } \partial E(t)$$

where v is the scalar velocity of $\partial E(t)$ along the normal direction.

Definition 2.4. Given $T > 0$, we say that a family $E(t)$, $t \in [0, T]$, is a *crystalline mean curvature flow in $[0, T]$ with forcing term $f \in L^\infty(\mathbb{R}^2)$* if:

- (i) $E(t) \subseteq \mathbb{R}^2$ is a Lipschitz set for every $t \in [0, T]$;
- (ii) There exists an open set $A \subseteq \mathbb{R}^2 \times [0, T]$ such that $\bigcup_{t \in [0, T]} \partial E(t) \times \{t\} \subseteq A$, and the function $d(\xi, t) \doteq d_\varphi^{E(t)}(\xi)$ is locally Lipschitz in A ;
- (iii) There exists a function $n \in L^\infty(A, \mathbb{R}^2)$, with $\operatorname{div} n \in L^\infty(A)$, such that the restriction of $n(t, \cdot)$ to $\partial E(t)$ is a Cahn-Hoffmann vector field for $\partial E(t)$ for every $t \in [0, T]$;
- (iv) $\partial_t d - \operatorname{div} n \in [f^-, f^+] \mathcal{H}^1$ -almost everywhere in $\partial E(t)$ and for all $t \in [0, T]$, where

$$f^+(\xi) = \operatorname{ess\,lim\,sup}_{\eta \rightarrow \xi} f(\eta), \quad f^-(\xi) = \operatorname{ess\,lim\,inf}_{\eta \rightarrow \xi} f(\eta), \quad \xi \in \mathbb{R}^2.$$

In general, the same φ -regular set E may admit more than one Cahn-Hoffmann vector field $n_\varphi \in \operatorname{Lip}(\partial E; \mathbb{R}^2)$. Most of these choices are meaningless from the point of view of the geometric evolution. In order to overcome this ambiguity we fix the choice by a variational selection principle which turns out to be consistent with the curve shortening flow (see [6–8, 26, 27]).

Definition 2.5 (Variational forced crystalline curvature flow). A *variational forced crystalline curvature flow* is a forced crystalline curvature flow $E(t)$, $t \in [0, T]$, such that for every $t \in [0, T]$ $n(t, \cdot)$ is the unique minimizer of the functional

$$\mathcal{N}(n) = \int_{\partial E(t)} |f - \operatorname{div} n|^2 d\mathcal{H}^1$$

in the set

$$D = \left\{ n \in L^\infty(\partial E(t), \mathbb{R}^2), n \in T_{\varphi^\circ}(\nabla d_\varphi^{E(t)}), \operatorname{div} n \in L^2(\partial E(t)) \right\}.$$

In Section 4 we will focus our attention to forced crystalline flows starting from *coordinate polyrectangles*; that is, Lipschitz polygonal domains whose boundary is a closed curve with edges parallel to the coordinate axes. In what follows the endpoints of an edge L of a coordinate polyrectangle will be called *vertices*.

We collect in the following proposition some basic properties of these planar sets (for details see, e.g., [5–8]).

Proposition 2.6. A coordinate polyrectangle E is a φ -regular set, and $T_{\varphi^\circ}(\nabla d_\varphi^E)$ is a fixed cone T_L in the interior of each edge L of ∂E . Moreover the following holds:

- (i) If p is a vertex of ∂E and L_1, L_2 are the edges of ∂E such that $L_1 \cap L_2 = \{p\}$, then $T_{L_1} \cap T_{L_2} = \{N_p\}$, and hence every Cahn-Hoffmann vector field $n \in \operatorname{Lip}(\partial E; \mathbb{R}^2)$ takes the value $n(p) = N_p$ at p ;

- (ii) *The restriction $n|_L$ to an edge L of the variational selection n obtained by minimization as in Definition 2.5 is the unique minimizer of the functional*

$$\mathcal{N}_L(n) = \int_L |f - \operatorname{div} n|^2 d\mathcal{H}^1$$

in the set

$$D_L = \left\{ n \in L^\infty(L, \mathbb{R}^2), \ n \in T_L, \ \operatorname{div} n \in L^2(L), \ n(p) = N_p, n(q) = N_q \right\}$$

where p, q are the endpoints of L and N_p, N_q are the values at the vertices p, q assigned by (i).

Note that, by classical elliptic regularity for Dirichlet problems, the minimizer in Proposition 2.6(ii) above belongs to the Sobolev space $H^2(L)$, and hence it is a Lipschitz function on L .

Remark 2.7. If the minimizer n_L in D_L of the functional \mathcal{N}_L satisfies the strict constraint $n_L(\xi) \in \operatorname{int}(T_L)$ for every $\xi \in L$, then the velocity $f - \operatorname{div} n_L$ is constant along the edge; that is, the flat arc remains flat under the evolution. This is always the case when $f = 0$, since the unique minimizer is the interpolation of the assigned values at the vertices of L , and the constant value of the mean φ -curvature is given by

$$\kappa_\varphi^L = \chi_L \frac{2}{\ell} \text{ on } L, \quad (2.2)$$

where ℓ is the length of the edge L and χ_L is a convexity factor: $\chi_L = 1, -1, 0$, depending on whether $E(t)$ is locally convex at L , locally concave at L , or neither.

We refer to [5, 19, 24] for some existence and uniqueness results for variational forced crystalline curvature flow, when the forcing term f is a Lipschitz function. To the best of our knowledge, there is no general results for discontinuous forcing terms.

The easiest example of variational forced crystalline curvature flow is the one starting from a coordinate rectangle R (rectangle with edges parallel to the coordinate axes), and with constant forcing term $f(\xi) = \gamma \in \mathbb{R}$.

Ordering the vertices of ∂E clockwise starting from the left-upper corner, P_i , $i \in \{1, \dots, 4\}$, we have

$$n_\varphi(P_1) = (-1, 1), \quad n_\varphi(P_2) = (1, 1), \quad n_\varphi(P_3) = (1, -1), \quad n_\varphi(P_4) = (-1, -1),$$

and hence the variational Cahn-Hoffmann vector field on the sides is

$$n_\varphi(\xi) = n_\varphi(P_i) + \frac{2(-1)^{i+1}}{\ell_i}(\xi - P_i), \quad \xi \in L_i, \ i \in \{1, \dots, 4\},$$

where L_i is the edge of the rectangle starting from P_i , and ℓ_i is its length.

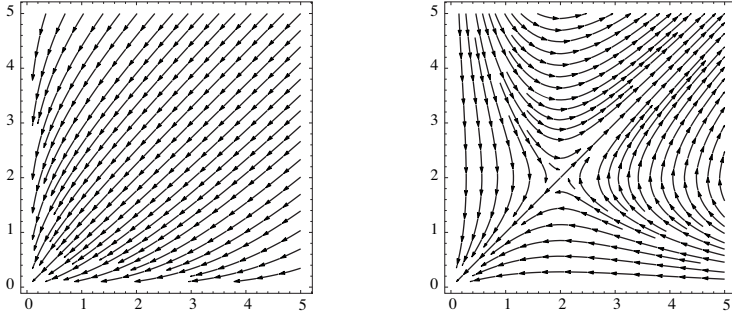


Figure 2.3. Phase portraits of (2.3) for $\gamma > 0$ and for $\gamma < 0$.

The φ -curvature associated to this field is constant on each edge L_i , and

$$\kappa_\varphi^i = \frac{2(-1)^{i+1}}{\ell_i} \text{ on } L_i, \quad i \in \{1, \dots, 4\}.$$

As a consequence the evolution of R is given by rectangles $R(t)$, and the description of the flow reduces to the analysis of a system of ODE's solved by the lengths $\ell_1(t)$ and $\ell_2(t)$ of the horizontal and the vertical edges of $R(t)$:

$$\begin{cases} \ell_1' = -\frac{4}{\ell_2} - 2\gamma \\ \ell_2' = -\frac{4}{\ell_1} - 2\gamma, \end{cases} \quad (2.3)$$

(see [1] and [25]). Hence, if $\gamma > 0$, ℓ_1 and ℓ_2 are decreasing functions, and we have finite-time extinction (see the phase portrait in the left-hand side of Figure 2.3), while if $\gamma < 0$ the evolution is the one depicted in the right-hand side of Figure 2.3. The square of side length $\ell^0 = -2/\gamma$ is the unique equilibrium of the system. Moreover, the function

$$U(\ell_1, \ell_2) = 4(\log(\ell_2) - \log(\ell_1)) + 2\gamma(\ell_2 - \ell_1)$$

is a constant of motion for the system (2.3). The squares starting with a side length shorter than ℓ^0 shrink to a point, while the squares starting with a side length longer than ℓ^0 expand with asymptotic velocity $-\gamma$ as the side length diverges. The rectangles can shrink to a point, converge to the equilibrium or expand, depending on the starting length of the edges.

In general, in presence of a spatially inhomogeneous forcing term, the selfsimilarity of the evolution of coordinate rectangles may fail, due to the possibility of edge breaking or bending phenomena (see [26, 27]).

2.4. The oscillating forcing term

In what follows we will consider a prototypical case of an oscillating layered forcing term: given two constants $\alpha < 0 < \beta$, we set

$$g(x) = \begin{cases} \alpha & \text{if } \text{dist}(x, \mathbb{Z}) \leq \frac{1}{4} \\ \beta & \text{otherwise,} \end{cases} \quad (2.4)$$

and we denote by \mathcal{I} the set of discontinuity lines of the function g :

$$\mathcal{I} := \left\{ (x, y), x \in \frac{1}{4} + \frac{1}{2}\mathbb{Z}, y \in \mathbb{R} \right\}.$$

In order to distinguish the two families of discontinuity lines for g , depending on the position of the phases α and β with respect to the interface, we will use the notation

$$\begin{aligned} \mathcal{I}_{\alpha, \beta} &:= \left\{ (x, y), y \in \mathbb{R}, x \in \mathbb{R} \text{ such that } g(s, y) = \beta \text{ for all } s \in \left(x, x + \frac{1}{2}\right) \right\} \\ \mathcal{I}_{\beta, \alpha} &:= \left\{ (x, y), y \in \mathbb{R}, x \in \mathbb{R} \text{ such that } g(s, y) = \alpha \text{ for all } s \in \left(x, x + \frac{1}{2}\right) \right\}. \end{aligned}$$

Given $\varepsilon > 0$ we consider the function g_ε defined by

$$g_\varepsilon(x, y) := g\left(\frac{x}{\varepsilon}\right),$$

(with an abuse of notation, we will often write $g_\varepsilon(x)$ instead of $g_\varepsilon(x, y)$). Setting

$$x_N := \left(N + \frac{1}{4}\right)\varepsilon, \quad N \in \mathbb{N}, \quad (2.5)$$

we have that

$$g_\varepsilon(x, y) = \begin{cases} \alpha & x \in \left(x_N - \frac{\varepsilon}{2}, x_N\right) \ y \in \mathbb{R} \\ \beta & x \in \left(x_N, x_N + \frac{\varepsilon}{2}\right) \ y \in \mathbb{R}; \end{cases} \quad (2.6)$$

that is, $\{x = x_N\} \subseteq \varepsilon \mathcal{I}_{\alpha, \beta}$ and $\{x = -x_N\} \subseteq \varepsilon \mathcal{I}_{\beta, \alpha}$ for every $N \in \mathbb{N}$ (see Figure 2.4).

Finally, we define the multifunction

$$G_\varepsilon(x, y) = \begin{cases} g_\varepsilon(x, y) & \text{if } (x, y) \notin \varepsilon \mathcal{I} \\ [\alpha, \beta] & \text{if } (x, y) \in \varepsilon \mathcal{I}. \end{cases}$$

With these definitions, a variational crystalline mean curvature flow $E(t)$ with forcing term g_ε has to have normal velocity $v(t) \in \text{div } n(t) + G_\varepsilon$ on $\partial E(t)$.

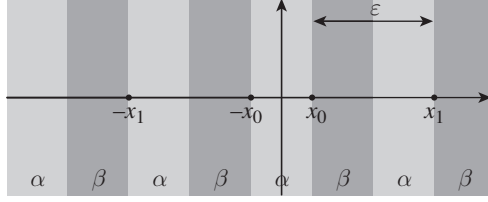


Figure 2.4. The oscillating forcing term g_ε .

3. Calibrable edges

In this section we keep $\varepsilon > 0$ fixed, and we focus our attention on the effect of the forcing term g_ε along the edges of a coordinate polyrectangle.

Definition 3.1. An edge L of a coordinate polyrectangle E is *calibrable* if there exist a Cahn-Hoffmann vector field n for ∂E and a constant $v \in \mathbb{R}$ such that $v \in \operatorname{div} n + G_\varepsilon$ on L . In this case we say that v is a (normal) *velocity of the edge* L .

Remark 3.2. In view of Proposition 2.6, in order to show that an edge L of ∂E is calibrable it is enough to show that there exists a vector field n on L , such that $n(\xi) \in T_L$ for every $\xi \in \operatorname{int} L$ and agrees with assigned values (prescribed by the geometry of ∂E) at the endpoints of L .

In what follows, the length of an edge L will be denoted by ℓ .

3.1. Vertical edges

Every vertical edge is calibrable. Namely, if $x = \bar{x} \in \mathbb{R}$ is the straight line containing L , there exists a constant selection $\gamma_\varepsilon(\bar{x})$ of G_ε on L , and hence the Cahn-Hoffman field given by the linear interpolation of the extreme values satisfies all the requirements. The related velocity of the edge is given by

$$v = \frac{2}{\ell} \chi_L + \gamma_\varepsilon(\bar{x}), \quad (3.1)$$

where χ_L is the convexity factor defined in Remark 2.7. Hence, the velocity of the edge is uniquely determined if L is not a subset of the jump set $\varepsilon \mathcal{I}$ of g_ε , while, for \bar{x} belonging to an interface we can freely choose any fixed value v such that

$$v \in \left[\frac{2}{\ell} \chi_L + \alpha, \frac{2}{\ell} \chi_L + \beta \right].$$

In particular, a vertical edge $L \subseteq \varepsilon \mathcal{I}$ with zero φ -curvature is allowed to have velocity zero, since we can choose $\gamma_\varepsilon = 0$ on L . Similarly, a vertical edge $L \subseteq \varepsilon \mathcal{I}$ either with positive φ -curvature and length $\ell \geq -2/\alpha$, or with negative φ -curvature and length $\ell \geq 2/\beta$ is allowed to have velocity zero, since we can choose $\gamma_\varepsilon = -2/\ell$ or $\gamma_\varepsilon = 2/\ell$ on L , respectively.

3.2. Horizontal edges

Let L be a horizontal edge. A Cahn-Hoffman vector field n_φ on L belongs to $T_{\varphi^\circ}(\nabla d_\varphi^E) = T_{\varphi^\circ}(\pm e_2)$, so that its second component is fixed (see (2.1)). In what follows we consider only its first component, by using the abuse of notation $n_\varphi = (n(x), \pm 1)$ on L .

Hence, $L = [p, q] \times \{\bar{y}\}$ turns out to be calibrable if there exists a Lipschitz function

$$n: [p, q] \rightarrow [-1, 1], \quad (3.2)$$

such that

$$n' + g_\varepsilon = \chi_L \frac{2}{\ell} + \frac{1}{\ell} \int_L g\left(\frac{s}{\varepsilon}\right) ds \quad \text{almost everywhere in } [p, q], \quad (3.3)$$

and with the following prescribed values at the endpoints

$$(BC) = \begin{cases} n(p) = n(q) = n_0 \in \{\pm 1\} & \text{if } \chi_L = 0 \\ n(p) = -1, n(q) = 1 & \text{if } \chi_L = 1 \\ n(p) = 1, n(q) = -1 & \text{if } \chi_L = -1. \end{cases} \quad (3.4)$$

Denoting by $\ell_\alpha, \ell_\beta \in [0, \varepsilon/2]$ the non-negative lengths given by the conditions

$$\ell - \varepsilon \left\lfloor \frac{\ell}{\varepsilon} \right\rfloor = \ell_\alpha + \ell_\beta, \quad \int_L g_\varepsilon(s) ds = \frac{\alpha + \beta}{2} (\ell - \ell_\alpha - \ell_\beta) + \alpha \ell_\alpha + \beta \ell_\beta, \quad (3.5)$$

the necessary condition (3.3) prescribes the value of n' outside the jump set of g_ε :

$$n'(x) = \begin{cases} \frac{1}{2\ell} (4\chi_L + (\beta - \alpha)(\ell - \ell_\alpha + \ell_\beta)) & \text{if } g_\varepsilon(x) = \alpha \\ \frac{1}{2\ell} (4\chi_L - (\beta - \alpha)(\ell + \ell_\alpha - \ell_\beta)) & \text{if } g_\varepsilon(x) = \beta, \end{cases} \quad (3.6)$$

and the velocity of the edge L :

$$v_L = \chi_L \frac{2}{\ell} + \frac{\alpha + \beta}{2} + \frac{\beta - \alpha}{2\ell} (\ell_\beta - \ell_\alpha). \quad (3.7)$$

In conclusion, the calibrability conditions (3.3) and (3.4) determine a candidate field n (and the related velocity of the edge), which is continuous and affine with given slope in each phase of g_ε . This field n is the Cahn-Hoffman field which calibrates L with velocity (3.7) if and only if it satisfies the constraint $|n(x)| \leq 1$ for every $x \in [p, q]$.

Remark 3.3. If $\ell > \varepsilon$, by (3.6) the variation of n in a period ε is

$$\Delta_\varepsilon n = n(x + \varepsilon) - n(x) = \frac{\varepsilon}{2\ell} (4\chi_L + (\beta - \alpha)(\ell_\beta - \ell_\alpha)). \quad (3.8)$$

In what follows we will assume

$$0 < \varepsilon < \frac{8}{\beta - \alpha}. \quad (3.9)$$

In particular, (3.9) implies that $\Delta_\varepsilon n$ has the sign of χ_L , and hence the constraint $|n| \leq 1$ is fulfilled in $[p, q]$ if it is satisfied in a suitable neighborhood of the extreme points p and q .

The calibrability of a horizontal edge L will depend on its length and on the position of its endpoints. We start by characterizing the calibrable horizontal edges with zero φ -curvature.

Proposition 3.4 (Horizontal edges with zero φ -curvature). *Let $L = [p, q] \times \{\bar{y}\}$ be a horizontal edge with zero φ -curvature, let ℓ_α, ℓ_β be the lengths defined in (3.5), and let $n_0 \in \{\pm 1\}$ be the given value of the Cahn-Hoffmann vector field at the endpoints of L . Then the following hold:*

- (i) *If $\ell = \ell_\alpha + \ell_\beta < \varepsilon$, L is calibrable with velocity $v_L = \frac{\alpha\ell_\alpha + \beta\ell_\beta}{\ell_\alpha + \ell_\beta}$ if and only if*
 - (ia) $n_0 = 1$, and either $g_\varepsilon(p) = \beta$, $g_\varepsilon(q) = \alpha$, or with an endpoint on $\varepsilon\mathcal{I}_{\alpha,\beta}$;
 - (ib) $n_0 = -1$, and either $g_\varepsilon(p) = \alpha$, $g_\varepsilon(q) = \beta$, or with an endpoint on $\varepsilon\mathcal{I}_{\beta,\alpha}$;
- (ii) *If $\ell \geq \varepsilon$, L is calibrable with velocity $v_L = \frac{\alpha+\beta}{2}$ if and only if*
 - (iia) $n_0 = 1$, and $(p, \bar{y}), (q, \bar{y}) \in \varepsilon\mathcal{I}_{\alpha,\beta}$;
 - (iib) $n_0 = -1$, and $(p, \bar{y}), (q, \bar{y}) \in \varepsilon\mathcal{I}_{\beta,\alpha}$.

Proof. We prove the case $n_0 = 1$, the other one being similar. By (3.6), the unique candidate field n is strictly increasing in every α phase, and strictly decreasing in every β phase, and, in order to satisfy the constraint $|n| \leq 1$ on L , the edge needs to be the union of three consecutive segments $L = L_\beta \cup L_c \cup L_\alpha$, with $L_\beta = [p, p + \ell_\beta] \times \{\bar{y}\}$, $L_c = [p + \ell_\beta, q - \ell_\alpha] \times \{\bar{y}\}$, $L_\alpha = [q - \ell_\alpha, q] \times \{\bar{y}\}$, with $p + \ell_\beta, q - \ell_\alpha \in \varepsilon\mathcal{I}_{\beta,\alpha}$. If $L_c = \emptyset$, then the constraint $|n| \leq 1$ is satisfied on L if and only if

$$-\ell_\beta \frac{\beta - \alpha}{2(\ell_\alpha + \ell_\beta)}(\ell + \ell_\alpha - \ell_\beta) = -\ell_\beta \ell_\alpha \frac{\beta - \alpha}{(\ell_\alpha + \ell_\beta)} \geq -2.$$

Under the assumption (3.9) this is always the case, since

$$(\beta - \alpha)\ell_\alpha\ell_\beta \leq \frac{8}{\varepsilon}\ell_\alpha\ell_\beta \leq 4\min\{\ell_\alpha, \ell_\beta\} \leq 2(\ell_\alpha + \ell_\beta),$$

proving (i).

On the other hand, if $L_c \neq \emptyset$, by (3.8) we have

$$n(p + \varepsilon) - n(p) = \frac{\varepsilon}{2\ell}(\beta - \alpha)(\ell_\beta - \ell_\alpha) = n(q) - n(q - \varepsilon),$$

and hence, since $n(p) = n(q) = 1$, the constraint $|n| \leq 1$ is not satisfied if $\ell_\alpha \neq \ell_\beta$. Finally, if $\ell_\alpha = \ell_\beta$, then

$$n'(x) = \begin{cases} \frac{\beta - \alpha}{2} & \text{if } g_\varepsilon(x) = \alpha, \\ \frac{\alpha - \beta}{2} & \text{if } g_\varepsilon(x) = \beta, \end{cases}$$

and a Canh-Hoffmann vector field with this derivative exists only if $\ell_\alpha = \ell_\beta = \varepsilon/2$, otherwise

$$n\left(p + \ell_\beta + \frac{\varepsilon}{2}\right) = 1 + \frac{\beta - \alpha}{2} \left(\frac{\varepsilon}{2} - \ell_\beta\right) > 1.$$

In conclusion, L is calibrable with velocity $v_L = (\alpha + \beta)/2$ if and only if $(p, \bar{y}), (q, \bar{y}) \in \varepsilon\mathcal{I}_{\alpha, \beta}$. \square

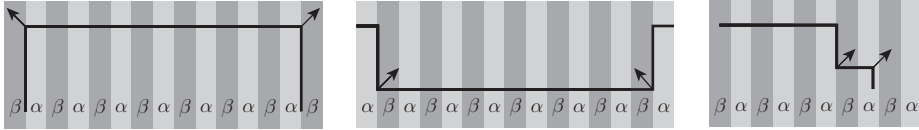


Figure 3.1. The calibrable edges in Propositions 3.7(i), 3.7(ii), and 3.4(ia).

Remark 3.5. If $L = [x_N, x_N + \delta] \times \{\bar{y}\}$, with $\bar{y} \in \mathbb{R}$, $\delta \in (0, \varepsilon)$, and x_N defined in (2.5), is a horizontal edge with zero φ -curvature (see Figure 3.1, right), then L is calibrable by Proposition 3.4(i). More precisely, if $\delta \leq \varepsilon/2$, then $g_\varepsilon = \beta$ on L , and we can take n constant on L , so that L has constant velocity $v_L = \beta$. On the other hand, if $\delta > \varepsilon/2$, then the field

$$n(x) = n(x_N) + \frac{\frac{\varepsilon}{2}\beta + (\delta - \frac{\varepsilon}{2})\alpha}{\delta}(x - x_N) - \int_{x_N}^x g_\varepsilon\left(\frac{s}{\varepsilon}\right) ds \quad (3.10)$$

calibrates the edge L with velocity

$$v_L = \frac{\frac{\varepsilon}{2}\beta + (\delta - \frac{\varepsilon}{2})\alpha}{\delta}, \quad \delta \in \left(\frac{\varepsilon}{2}, \varepsilon\right). \quad (3.11)$$

Concerning the edges with non zero φ -curvature, the following result shows that the edge is always calibrable when the curvature term is dominant.

Proposition 3.6. *Every horizontal edge L such that*

- (C₊) $\chi_L = 1$, and $\ell + \ell_\alpha - \ell_\beta \leq 4/(\beta - \alpha)$
- (C₋) $\chi_L = -1$, and $\ell - \ell_\alpha + \ell_\beta \leq 4/(\beta - \alpha)$

is calibrable with velocity v_L given by (3.7).

Proof. By (3.6), in both cases the candidate field n varies monotonically between the two extreme values: in the case (C_+) it is an increasing function from -1 to 1 , while in the case (C_-) it is a decreasing function from 1 to -1 . This ensures that the constraint (3.2) is satisfied. \square

When the forcing term dominates the curvature term, the calibrability may fail (see Proposition 3.10 below). Nevertheless, the edges with endpoints on suitable interfaces are always calibrable, as we show in the following result.

Proposition 3.7. *Let $L = [p, q] \times \{\bar{y}\}$ be a horizontal edge with $\ell \geq \varepsilon$. Then the following hold:*

(i) *If $\chi_L = 1$, $p \in \varepsilon\mathcal{I}_{\beta,\alpha}$, $q \in \varepsilon\mathcal{I}_{\alpha,\beta}$, then L is calibrable with velocity*

$$v_L = \frac{2}{\ell} + \frac{\alpha + \beta}{2} - \frac{(\beta - \alpha)\varepsilon}{4\ell};$$

(ii) *If $\chi_L = -1$, $p \in \varepsilon\mathcal{I}_{\alpha,\beta}$, $q \in \varepsilon\mathcal{I}_{\beta,\alpha}$, then L is calibrable with velocity*

$$v_L = -\frac{2}{\ell} + \frac{\alpha + \beta}{2} + \frac{(\beta - \alpha)\varepsilon}{4\ell}.$$

Proof. Assume that $\chi_L = 1$, $p \in \varepsilon\mathcal{I}_{\beta,\alpha}$, $q \in \varepsilon\mathcal{I}_{\alpha,\beta}$, so that $n(p) = -1$, $n(q) = 1$, $\ell_\alpha = \varepsilon/2$, and $\ell_\beta = 0$. Then, by (3.6), we have that the candidate Cahn-Hoffmann field n is increasing in $[p, p + \frac{\varepsilon}{2}]$, and, by (3.8) and (3.9),

$$n(p + \varepsilon) - n(p) = \frac{\varepsilon}{4\ell} (8 - (\beta - \alpha)\varepsilon) > 0.$$

Similarly, we have that n satisfies the constraint also in $[q - \varepsilon, q]$, and, again by (3.8), we conclude that $|n| \leq 1$ on L so that L is calibrable with velocity v_L given by (i). The proof of (ii) is similar. \square

Definition 3.8 (C-edges). We say that a horizontal edge $L = [p, q] \times \{\bar{y}\}$ is a C -edge if it is of one of the following types:

- (C^+) $\chi_L = 1$, $(p, \bar{y}) \in \varepsilon\mathcal{I}_{\beta,\alpha}$, $(q, \bar{y}) \in \varepsilon\mathcal{I}_{\alpha,\beta}$;
- (C^-) $\chi_L = -1$, $(p, \bar{y}) \in \varepsilon\mathcal{I}_{\alpha,\beta}$, $(q, \bar{y}) \in \varepsilon\mathcal{I}_{\beta,\alpha}$;
- (C^0) $\chi_L = 0$, and either $n_0 = 1$, and $(p, \bar{y}), (q, \bar{y}) \in \varepsilon\mathcal{I}_{\alpha,\beta}$, or $n_0 = -1$, and $(p, \bar{y}), (q, \bar{y}) \in \varepsilon\mathcal{I}_{\beta,\alpha}$.

By Propositions 3.4 and 3.7, every C -edge is calibrable.

Remark 3.9 (Symmetric C-edges). When L has positive φ -curvature, and $L = [-x_N, x_N] \times \{\bar{y}\}$, with $\bar{y} \in \mathbb{R}$ and x_N defined in (2.5), the velocity of L is given by

$$v_L = \frac{1}{x_N} + \frac{\alpha + \beta}{2} - \frac{(\beta - \alpha)\varepsilon}{8x_N}. \quad (3.12)$$

On the other hand, if L has negative φ -curvature, and $L = [-x_N - \frac{\varepsilon}{2}, x_N + \frac{\varepsilon}{2}] \times \{\bar{y}\}$, setting $\bar{x} = x_N + \frac{\varepsilon}{2}$, the velocity of L is given by

$$v_L = -\frac{1}{\bar{x}} + \frac{\alpha + \beta}{2} + \frac{(\beta - \alpha)\varepsilon}{8\bar{x}}. \quad (3.13)$$

We now state some general results concerning the long edges with positive φ -curvature.

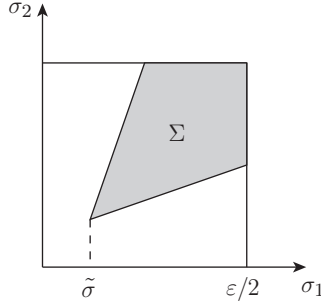


Figure 3.2. The calibrability set Σ in Proposition 3.10.

Proposition 3.10. *Let $L = [p, q] \times \{\bar{y}\}$ be a horizontal edge with positive φ -curvature, and such that $\ell + \ell_\alpha - \ell_\beta > 4/(\beta - \alpha)$. Then the following hold:*

- (i) *If either $g_\varepsilon(p) = \beta$, or $g_\varepsilon(q) = \beta$, or $p \in \varepsilon\mathcal{I}_{\alpha,\beta}$, or $q \in \varepsilon\mathcal{I}_{\beta,\alpha}$, then L is not calibrable;*
- (ii) *If $g_\varepsilon(p) = g_\varepsilon(q) = \alpha$, let $\sigma_1, \sigma_2 \in (0, \varepsilon/2)$ be such that $p + \frac{\varepsilon}{2} + \sigma_1 \in \varepsilon\mathcal{I}_{\beta,\alpha}$ and $q - \frac{\varepsilon}{2} - \sigma_2 \in \varepsilon\mathcal{I}_{\alpha,\beta}$, and let $\tilde{\ell}$ be the length of the interval $[p + \frac{\varepsilon}{2} + \sigma_1, q - \frac{\varepsilon}{2} - \sigma_2]$. Setting*

$$m = \varepsilon \frac{\beta - \alpha}{(\beta - \alpha)(\tilde{\ell} + \frac{\varepsilon}{2}) + 4}, \quad h = \frac{\varepsilon}{2} \frac{(\beta - \alpha)(\tilde{\ell} + \frac{\varepsilon}{2}) - 4}{(\beta - \alpha)(\tilde{\ell} + \frac{\varepsilon}{2}) + 4},$$

and

$$\Sigma = \left\{ (\sigma_1, \sigma_2) \in \mathbb{R}^2 : m\sigma_2 + h \leq \sigma_1 \leq \frac{1}{m}\sigma_2 - \frac{h}{m} \right\},$$

we have $m \in (0, 1)$, $\Sigma \cap [0, \varepsilon/2]^2 \neq \emptyset$, and L is calibrable with velocity

$$v_L = \frac{2}{\ell} + \frac{\alpha + \beta}{2} + \frac{\beta - \alpha}{2\ell} \left(\frac{\varepsilon}{2} - \sigma_1 - \sigma_2 \right)$$

if and only if $(\sigma_1, \sigma_2) \in \Sigma$;

- (iii) If $g_\varepsilon(p) = \alpha$, and $q \in \varepsilon\mathcal{I}_{\alpha,\beta}$ (resp. $p \in \varepsilon\mathcal{I}_{\beta,\alpha}$, and $g_\varepsilon(q) = \alpha$), let $\sigma \in (0, \frac{\varepsilon}{2})$ be such that $p + \sigma + \frac{\varepsilon}{2} \in \varepsilon\mathcal{I}_{\beta,\alpha}$, let ℓ^* be the length of the interval $[p + \frac{\varepsilon}{2} + \sigma, q]$ (respectively, of $[p, q - \frac{\varepsilon}{2} - \sigma]$), and let

$$\sigma^* = \frac{\varepsilon(\beta - \alpha)(\ell^* + \frac{\varepsilon}{2}) - 4}{2(\beta - \alpha)(\ell^* - \frac{\varepsilon}{2}) + 4}.$$

Then L is calibrable if and only if $\sigma \geq \sigma^*$.

Proof. If $\ell + \ell_\alpha - \ell_\beta > 4/(\beta - \alpha)$, by (3.6) the candidate Cahn-Hoffmann field n is strictly decreasing in the β phase. Hence, under the assumptions in (i), n does not satisfy the constraint $|n| \leq 1$ at least near an endpoint, and L is not calibrable.

Assume now that both the endpoints belong to the α phase, and let $\sigma_1, \sigma_2 \in (0, \varepsilon/2)$ be such that $p + \frac{\varepsilon}{2} + \sigma_1 \in \varepsilon\mathcal{I}_{\beta,\alpha}$ and $q - \frac{\varepsilon}{2} - \sigma_2 \in \varepsilon\mathcal{I}_{\alpha,\beta}$. Then, by (3.6), we have

$$\begin{aligned} n\left(p + \frac{\varepsilon}{2} + \sigma_1\right) - n(p) &= \sigma_1 \left(\frac{2}{\ell} + \frac{\beta - \alpha}{2\ell}(\ell + \ell_\beta - \ell_\alpha) \right) \\ &\quad + \frac{\varepsilon}{2} \left(\frac{2}{\ell} - \frac{\beta - \alpha}{2\ell}(\ell + \ell_\alpha - \ell_\beta) \right). \end{aligned}$$

In this case we have $\ell_\beta - \ell_\alpha = \frac{\varepsilon}{2} - \sigma_1 - \sigma_2$, and $\ell = \tilde{\ell} + \varepsilon + \sigma_1 + \sigma_2$, so that

$$\begin{aligned} &n\left(p + \frac{\varepsilon}{2} + \sigma_1\right) - n(p) \\ &= \sigma_1 \left(\frac{2}{\ell} + \frac{\beta - \alpha}{2\ell} \left(\tilde{\ell} + \frac{3}{2}\varepsilon \right) \right) + \frac{\varepsilon}{2} \left(\frac{2}{\ell} - \frac{\beta - \alpha}{2\ell} \left(\tilde{\ell} + \frac{\varepsilon}{2} + 2\sigma_1 + 2\sigma_2 \right) \right) \quad (3.14) \\ &= \frac{1}{2\ell} \left[\sigma_1 \left(4 + (\beta - \alpha) \left(\tilde{\ell} + \frac{\varepsilon}{2} \right) \right) + \frac{\varepsilon}{2} \left(4 - (\beta - \alpha) \left(\tilde{\ell} + \frac{\varepsilon}{2} + 2\sigma_2 \right) \right) \right]. \end{aligned}$$

Hence, if $\sigma_2 \geq \sigma_1 \geq m\sigma_2 + h$, we have

$$n\left(q - \frac{\varepsilon}{2} - \sigma_2\right) - n(q) \geq n\left(p + \frac{\varepsilon}{2} + \sigma_1\right) - n(p) \geq 0,$$

and n satisfies the constraint both in $[p, p + \frac{\varepsilon}{2} + \sigma_1]$ and in $[q - \frac{\varepsilon}{2} - \sigma_2, q]$. By Remark 3.3, we obtain that $|n| \leq 1$ on L , and hence L is calibrable. By symmetry, we obtain the same result when $\sigma_1 \geq \sigma_2 \geq m\sigma_1 + h$, and the conclusion follows.

Finally, we have that $m\sigma_2 + h = \sigma_1 = \frac{1}{m}\sigma_2 - \frac{h}{m}$ for $\sigma_1 = \sigma_2 = \tilde{\sigma}$, where

$$\tilde{\sigma} := \frac{\varepsilon(\beta - \alpha)(\tilde{\ell} + \frac{\varepsilon}{2}) - 4}{2(\beta - \alpha)(\tilde{\ell} - \frac{\varepsilon}{2}) + 4}, \quad (3.15)$$

and $\tilde{\sigma} \in (0, \varepsilon/2)$ under the assumption $\ell + \ell_\alpha - \ell_\beta > 4/(\beta - \alpha)$, so that $\Sigma \cap [0, \varepsilon/2]^2 \neq \emptyset$.

The proof of (iii) follows the same arguments. \square

Proposition 3.11. *Let $L = [p, q] \times \{\bar{y}\}$ be a horizontal edge with positive φ -curvature, and such that $\ell + \ell_\alpha - \ell_\beta > 4/(\beta - \alpha)$.*

Assume that $g_\varepsilon(p) = g_\varepsilon(q) = \alpha$, and that $p + \frac{\varepsilon}{2} + \sigma \in \varepsilon\mathcal{I}_{\beta,\alpha}$, $q - \frac{\varepsilon}{2} - \sigma \in \varepsilon\mathcal{I}_{\alpha,\beta}$ for a given $\sigma \in (0, \varepsilon/2)$, and let $\tilde{\ell}$ be the length of the interval $[p + \frac{\varepsilon}{2} + \sigma, q - \frac{\varepsilon}{2} - \sigma]$. Then L is calibrable if and only if $\sigma \geq \tilde{\sigma}$, where $\tilde{\sigma}$ is the value defined in (3.15). Moreover, if $\sigma = \tilde{\sigma}$, and n is the Cahn-Hoffmann vector field calibrating L , then

$$n(p) = n\left(p + \frac{\varepsilon}{2} + \tilde{\sigma}\right), \quad n(q) = n\left(q - \frac{\varepsilon}{2} - \tilde{\sigma}\right) \quad (3.16)$$

and

$$v_L = \frac{2}{\tilde{\ell}} + \frac{\alpha + \beta}{2} + \frac{\beta - \alpha}{2\tilde{\ell}} \left(\frac{\varepsilon}{2} - 2\tilde{\sigma} \right) = \frac{2}{\tilde{\ell}} + \frac{\alpha + \beta}{2} - \frac{(\beta - \alpha)\varepsilon}{4\tilde{\ell}} = \frac{\alpha\tilde{\sigma} + \beta\frac{\varepsilon}{2}}{\tilde{\sigma} + \frac{\varepsilon}{2}}. \quad (3.17)$$

Similarly, in the case (iii) of Proposition 3.10, when $\sigma = \sigma^*$, the edge L is calibrated by a Cahn-Hoffmann vector field n such that $n(p) = n(p + \frac{\varepsilon}{2} + \sigma^*)$, and

$$v_L = \frac{2}{\ell^*} + \frac{\alpha + \beta}{2} - \frac{(\beta - \alpha)\sigma^*}{2\ell^*} = \frac{2}{\ell^*} + \frac{\alpha + \beta}{2} - \frac{(\beta - \alpha)\varepsilon}{4\ell^*} = \frac{\alpha\sigma^* + \beta\frac{\varepsilon}{2}}{\sigma^* + \frac{\varepsilon}{2}}. \quad (3.18)$$

Proof. If $g_\varepsilon(p) = g_\varepsilon(q) = \alpha$, and $p + \frac{\varepsilon}{2} + \sigma \in \varepsilon\mathcal{I}_{\beta,\alpha}$, $q - \frac{\varepsilon}{2} - \sigma \in \varepsilon\mathcal{I}_{\alpha,\beta}$ for a given $\sigma \in (0, \varepsilon/2)$, then we are considering the case (ii) of Proposition 3.10 with $\sigma_1 = \sigma_2 = \sigma$. The calibrability condition $\sigma \geq \tilde{\sigma}$ then follows from the fact that $(\sigma, \sigma) \in \Sigma \cap [0, \varepsilon/2]^2$ if and only if $\sigma \in [\tilde{\sigma}, \varepsilon/2]$.

Moreover, the first equality in (3.16) follows from (3.14) with $\sigma_1 = \sigma_2 = \tilde{\sigma}$, while the second equality can be obtained with a similar argument.

Finally, (3.17) and (3.18) can be checked by a direct computation. \square

For the reader's convenience, we collect here the calibrability results in the case of symmetric edges with positive φ -curvature. In order to describe them, letting $x_N = (N + 1/4)\varepsilon$, $N \in \mathbb{N}$, we define $\bar{N}_\varepsilon \in \mathbb{N}$ by

$$\left(2x_N + \frac{\varepsilon}{2}\right) > \frac{4}{\beta - \alpha}, \quad \text{for all } N \geq \bar{N}_\varepsilon, \quad (3.19)$$

and $\delta(N) \in (0, \varepsilon)$ by

$$\delta(N) = \frac{x_N(\beta - \alpha)\varepsilon}{2 + \left(2x_N - \frac{\varepsilon}{2}\right) \frac{(\beta - \alpha)}{2}}, \quad (3.20)$$

then $\delta(N) > \varepsilon/2$ if and only if $N \geq \bar{N}_\varepsilon$.

Proposition 3.12 (Symmetric edges with positive φ -curvature). *Let*

$$L = [-\ell/2, \ell/2] \times \{\bar{y}\} \quad \ell > 0 \quad \bar{y} \in \mathbb{R},$$

be a horizontal edge with positive φ -curvature, and consider the decomposition $\ell/2 = x_{N_\varepsilon(\ell)} + \delta(\ell)$, with $0 \leq \delta(\ell) < \varepsilon$, and

$$N_\varepsilon(\ell) = \left\lfloor \frac{\ell}{2\varepsilon} - \frac{1}{4} \right\rfloor. \quad (3.21)$$

Then the following hold:

- (i) *If $N_\varepsilon(\ell) < \bar{N}_\varepsilon$, then the edge L is calibrable;*
- (ii) *If $N_\varepsilon(\ell) \geq \bar{N}_\varepsilon$ then the edge L is calibrable if and only if $\delta(\ell) \geq \delta(N_\varepsilon(\ell))$.*

Proof. Due to the very definition of \bar{N}_ε , if $N_\varepsilon(\ell) < \bar{N}_\varepsilon$ then L satisfies condition (C_+) of Proposition 3.6, and hence it is calibrable.

On the other hand, if $N_\varepsilon(\ell) \geq \bar{N}_\varepsilon$, then $\ell + \ell_\alpha - \ell_\beta > 4/(\beta - \alpha)$, and $\delta(N_\varepsilon(\ell)) = \tilde{\sigma} + \frac{\varepsilon}{2}$, where $\tilde{\sigma}$ is the calibrability threshold defined in (3.15). Then (ii) follows from Proposition 3.11. \square

We now state the analog of Proposition 3.10 for long edges with negative φ -curvature.

Proposition 3.13. *Let $L = [p, q] \times \{\bar{y}\}$ be a horizontal edge with negative φ -curvature, and such that $\ell + \ell_\beta - \ell_\alpha > 4/(\beta - \alpha)$. Then the following hold:*

- (i) *If either $g_\varepsilon(p) = \alpha$, or $g_\varepsilon(q) = \alpha$, or $p \in \varepsilon\mathcal{I}_{\beta,\alpha}$, or $q \in \varepsilon\mathcal{I}_{\alpha,\beta}$, then L is not calibrable;*
- (ii) *If $g_\varepsilon(p) = g_\varepsilon(q) = \beta$, let $\sigma_1, \sigma_2 \in (0, \varepsilon/2)$ be such that $p + \frac{\varepsilon}{2} + \sigma_1 \in \varepsilon\mathcal{I}_{\alpha,\beta}$ and $q - \frac{\varepsilon}{2} - \sigma_2 \in \varepsilon\mathcal{I}_{\beta,\alpha}$, and let $\tilde{\ell}$ be the length of the interval $[p + \frac{\varepsilon}{2} + \sigma_1, q - \frac{\varepsilon}{2} - \sigma_2]$. Then there exist $m \in (0, 1)$ and $h > 0$ such that L is calibrable with velocity*

$$v_L = -\frac{2}{\ell} + \frac{\alpha + \beta}{2} - \frac{\beta - \alpha}{2\ell} \left(\frac{\varepsilon}{2} - \sigma_1 - \sigma_2 \right)$$

- if and only if $(\sigma_1, \sigma_2) \in \{m\sigma_2 + h \leq \sigma_1 \leq \frac{1}{m}\sigma_2 - \frac{h}{m}\}$;*
- (iii) *If $g_\varepsilon(p) = \beta$, and $q \in \varepsilon\mathcal{I}_{\beta,\alpha}$ (resp. $p \in \varepsilon\mathcal{I}_{\alpha,\beta}$, and $g_\varepsilon(q) = \beta$), let $\sigma \in (0, \varepsilon/2)$ be such that $p + \sigma + \frac{\varepsilon}{2} \in \varepsilon\mathcal{I}_{\alpha,\beta}$, let ℓ^* be the length of the interval $[p + \frac{\varepsilon}{2} + \sigma, q]$ (respectively, of $[p, q - \frac{\varepsilon}{2} - \sigma]$), and let*

$$\sigma^* = \frac{\varepsilon(\beta - \alpha)(\ell^* + \frac{\varepsilon}{2}) - 4}{2(\beta - \alpha)(\ell^* - \frac{\varepsilon}{2}) + 4}.$$

Then L is calibrable if and only if $\sigma \geq \sigma^$.*

4. Effective motion as $\varepsilon \rightarrow 0$

4.1. Evolution of rectangles

In this section we consider evolutions starting from rectangular sets with edges parallel to coordinate axes. In what follows we will refer to them as “coordinate rectangles”.

Theorem 4.1 (Effective motion of coordinate rectangles). *Let R_0 be a coordinate rectangle, and let $\ell_{1,0}, \ell_{2,0}$ be the length of its horizontal and vertical edges, respectively. For every $\varepsilon > 0$, let R_0^ε be a coordinate rectangle such that $d_H(R_0, R_0^\varepsilon) < \varepsilon$. Then there exists a variational crystalline curvature flow of R_0^ε with forcing term g_ε . Moreover, every variational crystalline curvature flow $E^\varepsilon(t)$ of R_0^ε converges, in the Hausdorff topology and locally uniformly in time, as $\varepsilon \rightarrow 0$ to the coordinate rectangle $R(t)$ whose horizontal and vertical edges have lengths $\ell_1(t), \ell_2(t)$ solving the system of ODEs*

$$\begin{cases} \ell_1' = -2H_g(\ell_2) \\ \ell_2' = -\frac{4}{\ell_1} - (\alpha + \beta) \end{cases} \quad (4.1)$$

with initial datum $(\ell_1(0), \ell_2(0)) = (\ell_{1,0}, \ell_{2,0})$. The function $H_g(\ell): (0, +\infty) \rightarrow \mathbb{R}$ is a truncation of the harmonic mean defined by

$$H_g(\ell) := \begin{cases} 0 & \text{if } \ell \geq -\frac{2}{\alpha} \\ \left\langle \frac{2}{\ell} + g \right\rangle = \frac{1}{\int_0^1 \frac{1}{2/\ell_2 + g(s)} ds} = \frac{(2 + \alpha\ell_2)(2 + \beta\ell_2)}{\ell_2 \left(2 + \frac{\alpha + \beta}{2}\ell_2 \right)} & \text{otherwise.} \end{cases} \quad (4.2)$$

Remark 4.2. If we assume that the evolution $E^\varepsilon(t)$ of a coordinate rectangle R_0^ε is a coordinate rectangle for $t \in [0, T]$, and we denote by $(x_1(t), y_1(t)), (x_2(t), y_1(t)), (x_2(t), y_2(t)), (x_1(t), y_2(t))$, with $x_1(t) < x_2(t)$, and $y_1(t) > y_2(t)$, the coordinates of the vertices of $E^\varepsilon(t)$, the evolution of these points is governed by the system of ODEs

$$\begin{cases} x_1' = \frac{2}{y_1 - y_2} + g_\varepsilon(x_1) \\ x_2' = -\frac{2}{y_1 - y_2} - g_\varepsilon(x_2) \\ y_1' = -\frac{2}{x_2 - x_1} - \frac{\alpha + \beta}{2} - h_\varepsilon(y_1, y_2) \\ y_2' = \frac{2}{x_2 - x_1} + \frac{\alpha + \beta}{2} + h_\varepsilon(y_1, y_2) \end{cases} \quad (4.3)$$

in the domain $D := \{(x_1, x_2, y_2, y_1): x_1 < x_2, y_1 > y_2\}$. The Lipschitz function $h_\varepsilon: \{y_1 < y_2\} \subseteq \mathbb{R}^2 \rightarrow \mathbb{R}$ takes into account the small remainder varying in $[-\varepsilon/2, \varepsilon/2]$ and appearing in (3.7).

Applying the classical results of differential equations with discontinuous right-hand side (see [22, Chapter 2]), we obtain the following properties for the solutions:

- (i) For every $P_0 \in D$ there exists a (Filippov) solution to (4.3) starting from P_0 ;
- (ii) For every $P_0 \in D \cap \{y_1 - y_2 \leq -2/\alpha\}$ there exists a unique local solution to (4.3) starting from P_0 , and defined as long as it satisfies $y_1(t) - y_2(t) < -2/\alpha$;
- (iii) If $P_0 \in D \cap \{y_1 - y_2 > -2/\alpha\}$, the uniqueness of the solution starting from P_0 fails if and only if either x_1 or x_2 belongs to the set of “unstable discontinuities” $U = \{\pm(x_N + \frac{\varepsilon}{2}), N \in \mathbb{N}\}$ (see (3.21) for the definition of x_N). If this does not occur, then the solution is unique until the first time t_0 for which either $x_1(t_0)$ or $x_2(t_0)$ belong to U ;
- (iv) If $P_0 \in D \cap \{y_1 - y_2 > -2/\alpha\}$, and x_1 (respectively, x_2) belongs to the set of “stable discontinuities” $S = \{\pm x_N, N \in \mathbb{N}\}$, then $x'_1(t) = 0$ (respectively, $x'_2(t) = 0$) as long as the solution satisfies $y_1(t) - y_2(t) > -2/\alpha$.

Based on results of Section 3, a coordinate rectangle may not be calibrable, so that we cannot expect the evolution to preserve the geometry of the initial datum. In the proof of Theorem 4.1 we combine the previous properties of the solutions to (4.3) with a careful description of why and how the geometry changes during the evolution.

Proof of Theorem 4.1. We first assume that R_0 is centered at the origin. Using the notation

$$R(\ell_1, \ell_2) = \left[-\frac{\ell_1}{2}, \frac{\ell_1}{2} \right] \times \left[-\frac{\ell_2}{2}, \frac{\ell_2}{2} \right],$$

for this type of rectangles, $R_0 = R(\ell_{1,0}, \ell_{2,0})$.

We also assume that $R_0^\varepsilon = R(2x_{N_\varepsilon}, \ell_{2,0})$, where $N_\varepsilon = N_\varepsilon(\ell_{1,0})$ is defined in (3.21). In this case, recalling that the calibrability of a coordinate rectangle depends only on the calibrability of its horizontal edges (see Section 3.1), we have that R_0^ε is calibrable (see Remark 3.9), and the evolution starts according to (4.3).

Case 1 (homogenized velocities): $\ell_{1,0} < 4/(\beta - \alpha)$, $\ell_{2,0} \leq -2/\alpha$. The vertical edges of $R_0^\varepsilon = R(2x_{N_\varepsilon}, \ell_{2,0}^\varepsilon)$ are calibrable with velocity $v_2^\varepsilon(0) \geq 0$, and, by Remark 3.9, the horizontal edges are also calibrable with velocity

$$v_1^\varepsilon(0) = \frac{1}{x_{N_\varepsilon}} + \frac{\alpha + \beta}{2} + \frac{(\alpha - \beta)\varepsilon}{8x_{N_\varepsilon}} > 0.$$

Then, by Section 3.1, Proposition 3.6, and Remark 4.2(ii), the (unique) evolution is given by shrinking coordinate rectangles $R(\ell_1^\varepsilon(t), \ell_2^\varepsilon(t))$, and it is governed by system (4.3), or equivalently, by

$$\begin{cases} \ell_1^{\varepsilon'} = -\frac{4}{\ell_2^\varepsilon} - 2g\left(\frac{\ell_1^\varepsilon}{2\varepsilon}\right) \\ \ell_2^{\varepsilon'} = -\frac{4}{\ell_1^\varepsilon} - (\alpha + \beta) - \frac{(\alpha - \beta)\varepsilon}{2\ell_1^\varepsilon}. \end{cases} \quad (4.4)$$

In order to pass to the limit as $\varepsilon \rightarrow 0^+$ and to find the effective evolution, notice that $\ell_i^\varepsilon \in (\ell_{i,\beta}, \ell_{i,\alpha})$, for $i = 1$ or 2 , where $(\ell_{1,\alpha}, \ell_{2,\alpha})$ ($\ell_{1,\beta}, \ell_{2,\beta}$) are the solution to (2.3) with initial datum $(2x_{N_\varepsilon}, \ell_{2,0}^\varepsilon)$, and forcing term $\gamma = \alpha$ and $\gamma = \beta$ respectively. Hence, for $T > 0$, ℓ_i^ε are equilipschitz in $[0, T]$. Let $(\ell_1(t), \ell_2(t))$ be the uniform limit of a suitable subsequence of $(\ell_1^\varepsilon(t), \ell_2^\varepsilon(t))$ in $[0, T]$. Since $\ell_i(t)$ are a uniform limit of non-increasing functions, they are non-increasing and hence differentiable almost everywhere in $[0, T]$. Moreover, for $t \in (0, T)$ and $\sigma > 0$ such that $t + \sigma < T$, by the equilipschitz property of ℓ_2^ε we have $\ell_2^\varepsilon(\tau) = \ell_2^\varepsilon(t) + O(\sigma)$ for $\tau \in [t, t + \sigma]$ uniformly for ε small. Note that the velocity of each vertical side at time τ is then approximately equal to

$$\frac{2}{\ell_2^\varepsilon(t)} + g\left(\frac{\ell_1(\tau)}{2\varepsilon}\right)$$

up to $O(\sigma)$. If we consider a subinterval (τ_1, τ_2) of $(t, t + \sigma)$ where $g\left(\frac{\ell_1^\varepsilon(\cdot)}{2\varepsilon}\right)$ is constant, we may write

$$\tau_2 - \tau_1 = - \int_{\frac{\ell_1^\varepsilon(\tau_1)}{2}}^{\frac{\ell_1^\varepsilon(\tau_2)}{2}} \frac{1}{\frac{2}{\ell_2^\varepsilon(t)} + g\left(\frac{s}{2\varepsilon}\right)} ds + (\ell_1^\varepsilon(\tau_2) - \ell_1^\varepsilon(\tau_1))O(\sigma),$$

and hence, subdividing $(t, t + \sigma)$ into such intervals and summing the corresponding equalities, we obtain

$$\sigma = - \int_{\frac{\ell_1^\varepsilon(t)}{2}}^{\frac{\ell_1^\varepsilon(t+\sigma)}{2}} \frac{1}{\frac{2}{\ell_2^\varepsilon(t)} + g\left(\frac{s}{2\varepsilon}\right)} ds + (\ell_1^\varepsilon(t + \sigma) - \ell_1^\varepsilon(t))O(\sigma).$$

Denoting by $\langle (2/\ell_2(t)) + g \rangle$ the harmonic mean of $s \mapsto (2/\ell_2(t)) + g(s)$ for fixed t , letting $\varepsilon \rightarrow 0$ we deduce that

$$\sigma = - \int_{\frac{\ell_1(t)}{2}}^{\frac{\ell_1(t+\sigma)}{2}} \frac{1}{\langle (2/\ell_2(t)) + g \rangle} ds + o(\sigma),$$

or, in other terms that

$$\frac{\ell_1(t + \sigma) - \ell_1(t)}{\sigma} = -2 \left\langle \frac{2}{\ell_2(t)} + g \right\rangle + o(1). \quad (4.5)$$

If t is a differentiability point for ℓ_1 , from (4.5) it follows that $\ell_1'(t) = -2\langle (2/\ell_2(t)) + g \rangle$.

In conclusion, the effective evolution of the rectangle $R(\ell_{1,0}, \ell_{2,0})$ is given by rectangles $R(\ell_1(t), \ell_2(t))$ satisfying the evolution law

$$\begin{cases} \ell_1' = -2 \left\langle \frac{2}{\ell_2} + g \right\rangle \\ \ell_2' = -\frac{4}{\ell_1} - (\alpha + \beta). \end{cases} \quad (4.6)$$

In this case all the edges move inwards until a finite extinction time.

Case 2 (mesoscopic pinning): $\ell_{2,0} \geq -2/\alpha$. By Section 3.1, the vertical edges of $R_0^\varepsilon = R(2x_{N_\varepsilon}, \ell_{2,0})$ are calibrable with velocity $v_2^\varepsilon(0) = 0$. Moreover, by Proposition 3.7, the horizontal edges of $R_0^\varepsilon = (x_{N_\varepsilon}, \ell_{2,0})$ are also calibrable with velocity

$$v_1^\varepsilon(0) = \frac{1}{x_{N_\varepsilon}} + \frac{\alpha + \beta}{2} + \frac{(\alpha - \beta)\varepsilon}{8x_{N_\varepsilon}}.$$

If $v_1^\varepsilon(0) \leq 0$, then the length of the vertical edges does not decrease and the (unique) evolution at the mesoscopic scale is given by rectangles $R^\varepsilon(\ell_1^\varepsilon(t), \ell_2^\varepsilon(t))$, $t > 0$, where

$$\begin{cases} \ell_1^{\varepsilon'} = 0 \\ \ell_2^{\varepsilon'} = -\frac{2}{x_{N_\varepsilon}} - (\alpha + \beta) - \frac{(\alpha - \beta)\varepsilon}{4x_{N_\varepsilon}}. \end{cases}$$

Taking the limit as $\varepsilon \rightarrow 0$ we obtain that the effective evolution is given by $R(\ell_1(t), \ell_2(t))$, $t > 0$, where

$$\begin{cases} \ell_1' = 0 \\ \ell_2' = -\frac{4}{\ell_{1,0}} - (\alpha + \beta). \end{cases} \quad (4.7)$$

Hence, if $\alpha + \beta < 0$, the rectangles $R(-4/(\alpha + \beta), \ell_2)$ with $\ell_{2,0} \geq -2/\alpha$ are unstable equilibria, while, if $v_0 = 4/\ell_{1,0} + (\alpha + \beta) < 0$, the rectangle expands in the vertical direction with constant velocity v_0 , keeping the length of the horizontal edges fixed.

If, instead, $v_0 > 0$, then the horizontal edges start to move inward, so that the length of the vertical edges decreases, and (4.7) describes the evolution for $t \in [0, \bar{t}]$, where

$$\bar{t} = \sup\{t > 0: \ell_2(s) \geq -2/\alpha \text{ for all } s \in [0, t)\}.$$

Starting from $R(\ell_1(\bar{t}), -2/\alpha)$, the evolution is the one shown in Case 1 or 3, respectively.

Case 3 (mesoscopic breaking): $\ell_{1,0} \geq 4/(\beta - \alpha)$, $\ell_{2,0} \leq -2/\alpha$. By Section 3.1, the vertical edges of $R_0^\varepsilon = R(2x_{N_\varepsilon}, \ell_{2,0})$ are calibrable with velocity $v_2(0) \geq 0$, and, by Remark 3.9, the horizontal edges are calibrable with velocity

$$v_1^\varepsilon(0) = \frac{1}{x_{N_\varepsilon}} + \frac{\alpha + \beta}{2} + \frac{(\alpha - \beta)\varepsilon}{8x_{N_\varepsilon}}.$$

By Proposition 3.12, the evolution is a rectangle, with decreasing length of the horizontal edges $\ell_1^\varepsilon(t)$, until the time $t_\delta > 0$ such that $\ell_1^\varepsilon(t_\delta) = 2x_{N_\varepsilon} + 2\delta(N_\varepsilon - 1)$, where $\delta(N_\varepsilon - 1)$ is the calibrability threshold given in (3.20).

Notice that the evolution cannot continue as a rectangle for $t > t_\delta$, since the horizontal edges would not be calibrable after the time t_δ . However, by Proposition 3.11, the Cahn-Hoffman vector field calibrating the horizontal edges at time t_δ equals the one calibrating both the horizontal edges with positive φ -curvature

$$E_c^\pm := [-x_{N_\varepsilon-1}, x_{N_\varepsilon-1}] \times \{\pm \ell_2^\varepsilon(t_\delta)/2\}$$

with velocity

$$v_c^\varepsilon = \frac{1}{x_{N_\varepsilon-1}} + \frac{\alpha + \beta}{2} + \frac{(\alpha - \beta)\varepsilon}{8x_{N_\varepsilon-1}},$$

and the horizontal edges with zero φ -curvature

$$E_l^\pm := \left[\frac{-\ell_1(t_\delta)}{2}, -x_{N_\varepsilon-1} \right] \times \left\{ \pm \frac{\ell_2^\varepsilon(t_\delta)}{2} \right\}$$

$$E_r^\pm := \left[x_{N_\varepsilon-1}, \frac{\ell_1(t_\delta)}{2} \right] \times \left\{ \pm \frac{\ell_2^\varepsilon(t_\delta)}{2} \right\}$$

with the same velocity.

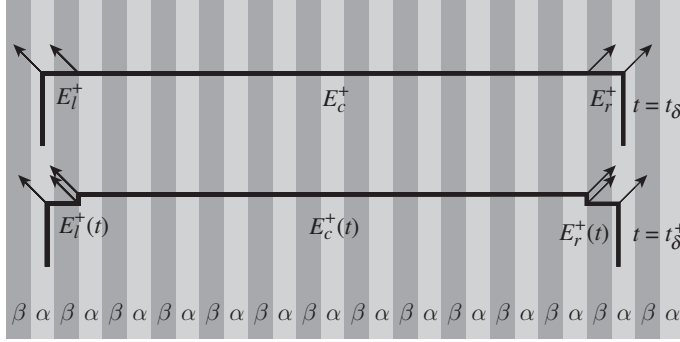


Figure 4.1. Breaking of the horizontal edge at $t = t_\delta$.

Hence, we can continue the evolution for $t > t_\delta$ by breaking the horizontal edges into three parts, that we denote by $E_l^\pm(t)$, $E_c^\pm(t)$ and $E_r^\pm(t)$ respectively, and inserting four vertical edges with zero φ -curvature at the breaking points. In this way, the evolving set becomes a coordinate polyrectangle $P^\varepsilon(t)$ (see Figure 4.1).

Notice that, by symmetry, the lengths and the velocities of the edges $E_l^\pm(t)$ and $E_r^\pm(t)$ are the same, and they will be denoted by $\ell_h^\varepsilon(t)$ and $v_h^\varepsilon(t)$, respectively.

By the discussion in Section 3.1 the small vertical edges with zero φ -curvature are pinned on the interfaces $x = \pm x_{N_\varepsilon-1}$, so that, by Remark 3.9, the long horizontal edges with positive φ -curvature $E_c^\pm(t)$ have constant length $\ell_1^\varepsilon = 2x_{N_\varepsilon-1}$, and move with velocity $v_1^\varepsilon(t) = v_c^\varepsilon$.

By Proposition 3.4(i) (see also Remark 3.5), the small horizontal edges $E_l^\pm(t)$ and $E_r^\pm(t)$ with zero φ -curvature and length $\ell_h^\varepsilon(t) \in (0, \frac{\varepsilon}{2} + \delta(N_\varepsilon))$ move with velocity $v_h^\varepsilon(t) > v_c^\varepsilon(t)$ given by

$$v_h^\varepsilon(t) = \begin{cases} \beta & \text{if } \ell_h^\varepsilon(t) \in (0, \varepsilon/2) \\ \frac{1}{\ell_h^\varepsilon(t)} \left(\frac{\varepsilon}{2} \beta + \left(\ell_h^\varepsilon(t) - \frac{\varepsilon}{2} \right) \alpha \right) & \text{if } \ell_h^\varepsilon(t) \in (\varepsilon/2, \varepsilon), \end{cases}$$

reducing the length $\ell_2^\varepsilon(t)$ of the long vertical edges with positive φ -curvature

$$\ell_2^\varepsilon(t) = \ell_2^\varepsilon(t_\delta) - \int_{t_\delta}^t v_h^\varepsilon(s) ds \leq \ell_2^\varepsilon(t_\delta) - v_c^\varepsilon(t - t_\delta).$$

On the other hand, the vertical long edges with positive φ -curvature move inward with velocity

$$v_2^\varepsilon(t) = \frac{2}{\ell_2^\varepsilon(t)} + g_\varepsilon \geq \frac{2}{\ell_2^\varepsilon(t_\delta) - v_c^\varepsilon(t - t_\delta)} + \alpha$$

so that, if we denote by t_1 the time when the vertical long edges with positive φ -curvature reach the interfaces $x = \pm x_{N_\varepsilon-1}$, we obtain

$$2\varepsilon \geq \int_{t_\delta}^{t_1} \frac{2}{\ell_2^\varepsilon(t_\delta) - v_c^\varepsilon(t - t_\delta)} dt + \alpha(t_1 - t_\delta) \geq \left(\frac{2}{\ell_2^\varepsilon(t_\delta)} + \alpha \right) (t_1 - t_\delta).$$

Hence, at $t = t_1$ the evolution is a rectangle $R(x_{N_\varepsilon-1}, \ell_2^\varepsilon(t_1))$ where

$$\ell_2^\varepsilon(t_1) = \ell_2^\varepsilon(t_\delta) - v_c^\varepsilon(t_1 - t_\delta) = \ell_2^\varepsilon(t_\delta) + O(\varepsilon), \quad \varepsilon \rightarrow 0^+.$$

The evolution then iterates this “breaking and recomposing” motion in such a way that it can be approximated, in the Hausdorff topology and locally uniformly in time, by a family of rectangles $R(\tilde{\ell}_1^\varepsilon(t), \tilde{\ell}_2^\varepsilon(t))$ satisfying (4.4), so that the effective motion is a family of rectangles $R(\ell_1(t), \ell_2(t))$ governed by the evolution law (4.6).

The general results recalled in Remark 4.2 can be used to show that the effective evolution (4.1) does not depend on the choice of the approximating sequence R_0^ε of initial data.

Namely, in Case 1, any coordinate rectangle R_0^ε is calibrable and the (unique) evolution starting from R_0^ε is the family of coordinate rectangles solving (4.3). This evolution has a distance of order ε from the one starting from $R(2x_{N_\varepsilon}, \ell_{2,0})$ uniformly in time, so that it converges, as $\varepsilon \rightarrow 0^+$ to the same effective evolution.

Similarly, in Case 3, we have that the evolution starting from R_0^ε becomes a rectangle with vertical edges with left endpoint on $\varepsilon \mathcal{I}_{\beta,\alpha}$ and right endpoint on $\varepsilon \mathcal{I}_{\alpha,\beta}$ in a time span of order ε , possibly breaking and recomposing the horizontal edges in the meanwhile. Then, the effective evolution of R_0 is uniquely determined by (4.6).

On the other hand, if $\ell_{2,0} > -2/\alpha$, then, by Remark 4.2(iii) and (iv), the position of the vertical edges during the evolution is confined in the strip $\{x \in [x_{N_\varepsilon-1}, x_{N_\varepsilon}]\}$, with $N_\varepsilon = N_\varepsilon(\ell_{1,0}^\varepsilon)$. Hence, at a macroscopic level, the vertical edges are pinned, and the effective evolution of R_0 is uniquely determined by (4.7). \square

System (4.1) is integrable, and its phase portrait is plotted in Figure 4.2. Notice the pinning effect for long vertical edges, and the presence of a half line of nontrivial equilibria for $\alpha + \beta < 0$.

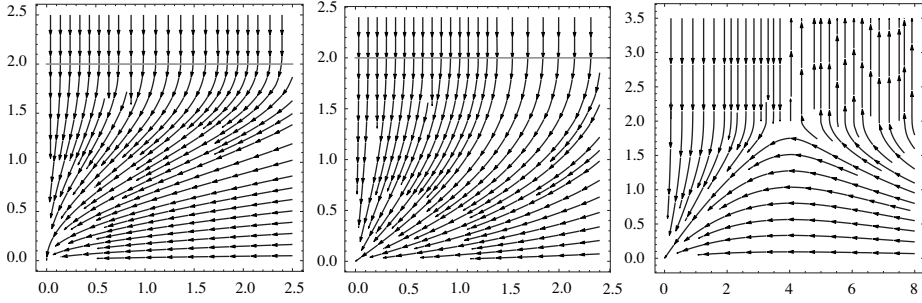


Figure 4.2. Phase portraits of (4.1) for $\alpha + \beta = 0$ (left), > 0 (center), < 0 (right).

4.2. Evolution of polyrectangles

We now extend the previous results to the more general class of *coordinate polyrectangles*; that is, those Lipschitz sets whose boundary is a closed polygonal curve with edges parallel to the coordinate axes.

Given a coordinate polyrectangle E , in what follows we will denote by H^0 , H^+ , and H^- (respectively, V^0 , V^+ , and V^-) the sets of the horizontal (respectively, vertical) edges of ∂E with zero, positive and negative φ -curvature. Moreover we set $H = H^0 \cup H^+ \cup H^-$, and $V = V^0 \cup V^+ \cup V^-$.

In what follows ℓ will denote the length of the edge L .

Remark 4.3. Given a coordinate polyrectangle E , the description of the variational crystalline curvature flow $E^\varepsilon(t)$ with forcing term g_ε starting from E will be obtained by combining the calibrability properties of the edges proved in Section 3 and information about solutions of a coupled system of ODEs solved by the coordinates of the vertices of $E(t)$ in any interval I in which the number of vertices of $E^\varepsilon(t)$ does not change.

More precisely, let $(x_i(t), y_i(t))$, $i \in \{1, \dots, N\}$, be the coordinates of the vertices of the polyrectangles $E^\varepsilon(t)$, $t \in I$, ordered clockwise in such a way that

$$\begin{aligned} (x_1, y_1) &= (x_{N+1}, y_{N+1}) & x_{2k}(t) &= x_{2k+1}(t) \\ y_{2k}(t) &= y_{2k-1}(t) & k \in \left\{1, \dots, \frac{N}{2}\right\} & t \in I, \end{aligned}$$

and the edges of $E^\varepsilon(t)$ are given by

$$L_i(t) = \begin{cases} [x_i(t), x_{i+1}(t)] \times \{y_i\} & \text{for } i \text{ odd} \\ \{x_i\} \times [y_i(t), y_{i+1}(t)] & \text{for } i \text{ even.} \end{cases}$$

Then $(x_1(t), \dots, x_N(t), y_1(t), \dots, y_N(t))$ is a solution in I to the system of ODEs

$$\begin{cases} x'_{2k} = x'_{2k+1} = -\frac{2}{y_{2k} - y_{2k+1}} \chi_{L_{2k}} - g_\varepsilon(x_{2k}) \\ y'_{2k} = y'_{2k+1} = -\frac{1}{x_{2k} - x_{2k-1}} \left(2\chi_{L_{2k-1}} + \int_{x_{2k-1}}^{x_{2k}} g_\varepsilon(s) ds \right) \end{cases} \quad k \in \left\{ 1, \dots, \frac{N}{2} \right\}. \quad (4.8)$$

The velocity field in (4.8) is discontinuous on the set

$$\mathcal{D} := \{(x_1, \dots, x_N, y_1, \dots, y_N) : i \in \{1, \dots, N\} \text{ exists, such that } x_i \in \varepsilon\mathcal{I}\},$$

so that the discontinuities only affect the motion of the vertical edges. We collect here the main features of the solutions to (4.8) (see [22, Chapter 2]), written in terms of motion of the edges of $\partial E^\varepsilon(t)$, $t \in I$. Since the system (4.8) is autonomous, it is enough to discuss the properties of local solutions starting from given datum E .

- (i) Pinning effect (stable discontinuities). Let $\ell_p > 0$ be the pinning threshold defined by

$$\ell_p = \begin{cases} -\frac{2}{\alpha}, & \text{if } L \in V^+ \\ 0, & \text{if } L \in V^0 \\ \frac{2}{\beta}, & \text{if } L \in V^-. \end{cases}$$

Then every vertical edge $L \in \partial E$ with $\ell > \ell_p$ and such that either $v(L) = e_1$ and $L \in \varepsilon\mathcal{I}_{\beta,\alpha}$ or $v(L) = -e_1$ and $L \in \varepsilon\mathcal{I}_{\alpha,\beta}$ is pinned during the evolution $E^\varepsilon(t)$ for every $t > 0$ such that $\ell(t) \geq \ell_p$;

- (ii) Transversality condition. The motion of a vertical edge $L \in V^- \cup V^+$ with $\ell < \ell_p$ is uniquely determined until $\ell(t) < \ell_p$;
- (iii) Uniqueness condition (unstable discontinuities). The uniqueness of the local solution starting from E fails if and only if there is a vertical edge $L \in V^- \cup V^+$ with $\ell > \ell_p$ and such that either $v(L) = e_1$ and $L \in \varepsilon\mathcal{I}_{\alpha,\beta}$ or $v(L) = -e_1$ and $L \in \varepsilon\mathcal{I}_{\beta,\alpha}$ (unstable edges). If this does not occur, the solution is unique until the first time t_0 when $E^\varepsilon(t_0)$ has a unstable edge.

A significant class of coordinate polyrectangles with a well-posed forced evolution is the following (see Proposition 4.7 and Theorem 4.8 below).

Definition 4.4 (\mathcal{C} -polyrectangles). Given $\varepsilon > 0$, we say that a coordinate polyrectangle E is a \mathcal{C} -polyrectangle if every horizontal edge of E is a \mathcal{C} -edge (see Definition 3.8).

Remark 4.5. By Proposition 3.7, Proposition 3.4, and Remark 4.3, every \mathcal{C} -polyrectangle is calibrable, with velocity of an edge L given by

$$v_L = \begin{cases} \frac{\alpha + \beta}{2} + \chi_L \left(\frac{2}{\ell} - \frac{(\beta - \alpha)\varepsilon}{4\ell} \right) & L \in H \\ \frac{2}{\ell} \chi_L + \gamma_\varepsilon & L \in V^+ \cup V^-, \ell < \ell_p \\ 0 & L \in V^0, \text{ and } L \in V^- \cup V^+ \text{ with } \ell \geq \ell_p, \end{cases} \quad (4.9)$$

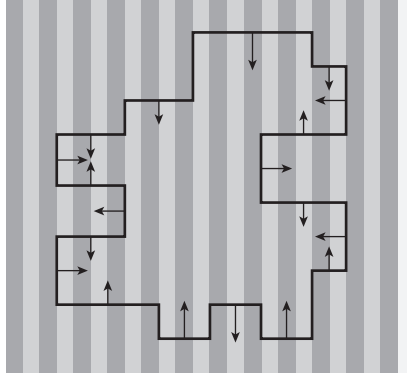


Figure 4.3. A \mathcal{C} -polyrectangle with velocities of its edges (case $\alpha + \beta > 0$).

(see Figure 4.3), and the variational crystalline curvature flow with forcing term g_ε of E starts following the rules (4.8). In particular, every edge $L \in V^0$ is pinned, as well as any edge $L \in V^- \cup V^+$ with length $\ell \geq \ell_p$.

Theorem 4.6 (Effective motion of coordinate polyrectangles). *Let E_0 be a coordinate polyrectangle. For $\varepsilon > 0$, let E_0^ε be a coordinate polyrectangle such that $d_H(E_0, E_0^\varepsilon) < \varepsilon$. Then there exists a variational crystalline curvature flow with forcing term g_ε starting from E_0^ε . Moreover, there exists a family of coordinate polyrectangles $E(t)$ such that every variational crystalline curvature flow $E^\varepsilon(t)$ with forcing term g_ε starting from E_0^ε converges to $E(t)$ in the Hausdorff topology and locally uniformly in t , for $\varepsilon \rightarrow 0$.*

Denoting by $\ell(t)$ the length of an edge $L(t) \subseteq \partial E(t)$, the normal velocity $v_L(t)$ of $L(t)$ is given by

$$v_L(t) = \begin{cases} \left\langle g + \frac{2}{\ell(t)} \right\rangle & \text{if } L(t) \in V^+, \text{ and } \ell(t) < -2/\alpha \\ \left\langle g - \frac{2}{\ell(t)} \right\rangle & \text{if } L(t) \in V^-, \text{ and } \ell(t) < 2/\beta \\ 0 & \text{for the other vertical edges} \\ \frac{2}{\ell(t)} \chi_L + \frac{\alpha + \beta}{2} & \text{if } L(t) \text{ is horizontal.} \end{cases} \quad (4.10)$$

The dynamics (4.10) is valid until $\ell(t) > 0$. If an edge vanishes at $t = t_0$, the evolution proceeds reinitializing the ODEs by starting from $E(t_0)$.

Proof. The existence of a variational crystalline curvature flow with forcing term g_ε starting from a coordinate polyrectangle E_0^ε and the fact that the effective evolution does not depend on the choice of the approximating data can be obtained with arguments similar to the ones proposed in detail in Section 4.1. We roughly sketch here the main features of such an evolution starting from a \mathcal{C} -polyrectangle E_0^ε .

By Remark 4.5, the “long” vertical edges of ∂E_0^ε with non zero φ -curvature, and all the vertical edges with zero φ -curvature are pinned. The vertical edges in V^+ with length $\ell < -2/\alpha$ move inward, while the vertical edges in V^- with length $\ell < 2/\beta$ move outward.

By Proposition 3.4, every edge $L \in H^0$ with pinned vertices has velocity $(\alpha + \beta)/2$, while every edge $L \in H^0$ with an adjacent moving vertical edge breaks instantaneously in a small part L_ε with length ε , and a remaining part calibrated with velocity $(\alpha + \beta)/2$. During the evolution L_ε shrinks and disappears in a time of order ε , while the remaining part has pinned vertices and moves vertically with velocity $(\alpha + \beta)/2$.

Similarly, every edge $L \in H^+ \cup H^-$ with pinned vertices has velocity given by (4.9), while every edge $L \in H^+ \cup H^-$ with an adjacent moving vertical edge shrinks until the calibrability conditions of Propositions 3.10 and 3.13 hold, and possibly it breaks following the rules of Proposition 3.11.

In any case, the possible “breaking and recomposing” motion occurs in a lapse of time of order ε , so that the evolution $E^\varepsilon(t)$ can be approximated by a family of \mathcal{C} -polyrectangles $\tilde{E}^\varepsilon(t)$ converging as $\varepsilon \rightarrow 0$ to a coordinate polyrectangle $E(t)$ in Hausdorff topology and locally uniformly in time. The effective velocities (4.10) of the edges of $E(t)$ are obtained taking the limit, as $\varepsilon \rightarrow 0$ in (4.9). In particular, the arguments for getting the velocities of the “short” vertical edges are the same of Case 1 in Section 4.1. \square

The variational crystalline curvature flow with forcing term g_ε starting from a \mathcal{C} -polyrectangle is unique and satisfies a comparison principle.

Proposition 4.7 (Uniqueness). *Given $\varepsilon > 0$, the variational crystalline curvature flow $E^\varepsilon(t)$ with forcing term g_ε starting from a \mathcal{C} -polyrectangle E is unique.*

Proof. By Remark 4.3(iii), uniqueness may fail if and only if there exists $t_0 > 0$ such that $\partial E(t_0)$ has a unstable edge. We will show that this never occurs when the initial datum E is a \mathcal{C} -polyrectangle.

By Remarks 4.3 and 4.5, the evolution starts with all the vertical edges pinned on interfaces in $\varepsilon\mathcal{I}$ that are stable equilibria of the dynamics, except for the “short” edges with nonzero φ -curvature. Moreover, the evolution may generate, for $t > 0$ new vertical edges, due to the breaking phenomenon of the horizontal edges. Nevertheless, every new vertical edge L belongs to V^0 and it is pinned on a stable discontinuity of g_ε .

Hence, if we assume by contradiction that there exists $t_0 > 0$ such that $\partial E(t_0)$ has a unstable edge, then it is the evolution $L(t_0)$ of a “short” edge (that is, $L \in V^- \cup V^+$ with $\ell < \ell_p$) enlarging during the evolution. More precisely, if we assume that $L(t_0) \in V^+$ and $\nu(L(t_0)) = e_1$ (the other cases being similar), the following properties should be satisfied:

$$L(t_0) \in \varepsilon\mathcal{I}_{\alpha,\beta}, \quad \ell(t_0) > -2/\alpha,$$

and there exists $\sigma > 0$ such that

$$g_\varepsilon = \alpha \text{ on } L(t) \text{ for } t \in (t_0 - \sigma, t_0), \quad \ell(t_0 - \sigma) < -2/\alpha.$$

Since $\partial E(t_0)$ needs to be calibrable, the horizontal edges adjacent to $L(t_0)$ have either zero φ -curvature, length $\varepsilon/2$ and velocity β , or positive φ -curvature, and length satisfying $\ell + \ell_\alpha - \ell_\beta \leq 4/(\beta - \alpha)$ (see Proposition 3.6), and hence velocity

$$v = \frac{2}{\ell} + \frac{\alpha + \beta}{2} + \frac{\beta - \alpha}{2\ell}(\ell_\beta - \ell_\alpha) = \frac{1}{2\ell}(4 - (\beta - \alpha)(\ell + \ell_\alpha - \ell_\beta) + 2\beta\ell) > 0.$$

In both cases the horizontal edges adjacent to $L(t_0)$ have strictly positive velocity, in contradiction with the fact that $L(t)$ enlarges for $t < t_0$ close enough to t_0 . \square

Theorem 4.8 (Comparison for forced flows). *For a given $\varepsilon > 0$, let E and F be two \mathcal{C} -polyrectangles such that $E \subseteq F$, and let $E^\varepsilon(t)$, $F^\varepsilon(t)$ be the variational crystalline curvature flow of E and F , respectively, with forcing term g_ε . Then*

- (i) $E^\varepsilon(t) \subseteq F^\varepsilon(t)$ for every t ;
- (ii) The distance $d^\varepsilon(t)$ between $\partial E^\varepsilon(t)$ and $\partial F^\varepsilon(t)$ satisfies

$$d^\varepsilon(t) \geq d^\varepsilon(0) \text{ for all } t \geq 0, \text{ and } d^\varepsilon(t_1) \geq d^\varepsilon(t_2) - \varepsilon \text{ for all } t_1 \geq t_2 > 0.$$

Proof. Given $\sigma > 0$, let $E_\sigma^\varepsilon(t)$ be the variational crystalline curvature flow of E with forcing term $g_\varepsilon + \sigma$. Following the proof of the First Comparison Principle in [25], mainly based on geometric arguments, we obtain that $E_\sigma^\varepsilon(t) \subseteq F^\varepsilon(t)$.

Moreover, by Theorem 4.6, Proposition 4.7, and in [22, Theorem 2.8.2], we infer that for every $n \in \mathbb{N}$ there exists $\sigma_n > 0$ such that, for every $t > 0$, the evolutions $E_{\sigma_n}^\varepsilon(t)$ converge, as $n \rightarrow +\infty$, in the Hausdorff topology to the variational crystalline curvature flow $E^\varepsilon(t)$ with forcing term g_ε starting from E . Hence, (i) follows from a passage to the limit for the inclusions $E_{\sigma_n}^\varepsilon(t) \subseteq F^\varepsilon(t)$.

In order to prove (ii), we underline that for every $t > 0$ the minimal distance $d(t)$ between $\partial E^\varepsilon(t)$ and $\partial F^\varepsilon(t)$ is attained at points joined by a segment parallel to a coordinate axis, so that either $E(t) + d(t)e_1 \subseteq F(t)$ or $E(t) + d(t)e_2 \subseteq F(t)$. On the other hand, since E is a \mathcal{C} -polyrectangle, we have that, for every $\gamma \in \mathbb{R}$, $E^\varepsilon(t) + \gamma e_2$ is the variational crystalline curvature flow with forcing term g_ε starting from $E + \gamma e_2$, and, for every $k \in \mathbb{Z}$, $E^\varepsilon(t) + k\varepsilon e_1$ is the variational crystalline curvature flow with forcing term g_ε starting from $E + k\varepsilon e_1$.

Let $t_1 \geq 0$ be given. If $E(t_1) + d(t_1)e_2 \subseteq F(t_1)$, then, by (i) and the invariance of the flow under vertical translations, we have that $E(t) + d(t_1)e_2 \subseteq F(t)$, and hence $d^\varepsilon(t_1) \geq d^\varepsilon(t)$, for every $t \geq t_1$. If, instead, $E(t_1) + d(t_1)e_1 \subseteq F(t_1)$, with the same argument we obtain that (ii) holds and that $d^\varepsilon(t_1) \geq d^\varepsilon(t)$ for every $t \geq t_1$ if and only if $d(t_1) = k\varepsilon$. \square

4.3. Evolution of more general sets

The macroscopic effect of the underlying oscillating forcing term g_ε on the crystalline curvature flow starting from any smooth, connected bounded set C_0 may be captured in the following way.

For every $\varepsilon > 0$, let \mathcal{C}_ε be the set of all \mathcal{C} -polyrectangles. For every $E_\varepsilon(0) \in \mathcal{C}_\varepsilon$, let $E_\varepsilon(t)$ be the unique variational crystalline curvature flow with forcing term g_ε starting from $E_\varepsilon(0)$. We define the families of sets

$$C_\varepsilon^+(t) = \bigcap_{\substack{C_0 \subseteq P_\varepsilon(0) \\ P_\varepsilon(0) \in \mathcal{C}_\varepsilon}} P_\varepsilon(t), \quad C_\varepsilon^-(t) = \bigcup_{\substack{Q_\varepsilon(0) \subseteq C_0 \\ Q_\varepsilon(0) \in \mathcal{C}_\varepsilon}} Q_\varepsilon(t),$$

and

$$C^+(t) = \limsup_{\varepsilon \rightarrow 0^+} C_\varepsilon^+(t) = \bigcap_{\eta > 0} \left(\bigcup_{0 < \varepsilon < \eta} C_\varepsilon^+(t) \right),$$

$$C^-(t) = \liminf_{\varepsilon \rightarrow 0^+} C_\varepsilon^-(t) = \bigcup_{\eta > 0} \left(\bigcap_{0 < \varepsilon < \eta} C_\varepsilon^-(t) \right).$$

By Theorem 4.8, for every $P_\varepsilon(0), Q_\varepsilon(0) \in \mathcal{C}_\varepsilon$ such that $Q_\varepsilon(0) \subseteq C_0 \subseteq P_\varepsilon(0)$, the evolutions satisfy $Q_\varepsilon(t) \subseteq P_\varepsilon(t)$ for every $t \geq 0$. Hence, we have $C_\varepsilon^-(t) \subseteq C_\varepsilon^+(t)$, $t \geq 0$.

Moreover, denoting by $P(t), Q(t)$ the effective evolution starting from coordinate polyrectangles $P(0), Q(0)$, and evolving with the law (4.10), by Theorem 4.6 we obtain that

$$\bigcup_{Q(0) \subseteq C_0} Q(t) \subseteq C^-(t) \subseteq C^+(t) \subseteq \bigcap_{C_0 \subseteq P(0)} P(t) \quad t \geq 0.$$

Notice that $C^-(0) = C^+(0) = C_0$. When $C^-(t) = C^+(t) =: C(t)$ for $t > 0$, this procedure defines the limit evolution starting from C_0 and driven, at a mesoscopic scale, by crystalline curvature flow with forcing term g_ε .

If C_0 is a bounded convex subset of \mathbb{R}^2 with nonempty interior, then $C^-(t) = C^+(t)$ for all $t \geq 0$, and we can explicitly describe the motion $C(t)$ starting from C_0 .

Approximation far from the “extreme points”: constant vertical shift. Let $\xi \in \partial C_0$ be such that $\nu(\xi)$ is not a coordinate vector. In this case, we can choose approximating sequences of \mathcal{C} -polyrectangles with all edges with zero φ -curvature in a suitable neighborhood of ξ (see Figure 4.4, left). The evolution by (4.10) of such an approximation is the following: the vertical edges are pinned, while the horizontal edges move with velocity $(\alpha + \beta)/2$. At a macroscopic level, the effect is a vertical motion of ∂C_0 near ξ with velocity $(\alpha + \beta)/2$.

Approximation near the “extreme points”: flat evolution. Let $\xi \in \partial C_0$ be such that $\nu(\xi) = \pm e_1$. In this case, we can choose approximating sequences of \mathcal{C} -polyrectangles with one horizontal edge with positive φ -curvature in a suitable neighborhood of ξ . Then the evolution $C(t), t > 0$, has a horizontal edge $L(t)$ with length $l(t)$ moving vertically with velocity $2/\ell(t) + (\alpha + \beta)/2$. The same arguments show that the evolution $C(t), t > 0$, has flat vertical edges “generated by” the points

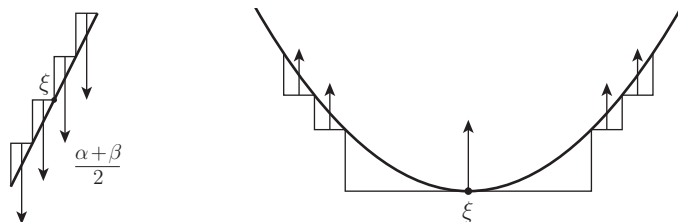


Figure 4.4. Approximation far from (left) and near to (right) an extreme point.

$\xi \in \partial C_0$ be such that $\nu(\xi) = \pm e_2$ and moving horizontally with velocity $H_g(\ell(t))$ (see (4.2)).

In conclusion, the effective evolution $C(t)$ of a convex set C_0 can be depicted as follows.

- The arcs with zero φ -curvature moves vertically with velocity $(\alpha + \beta)/2$. We denote by $C_1(t)$ the set obtained with this translation;
- There is an instantaneous generation of four flat edges parallel to the coordinate axes and with the extreme points constrained on the set $C_1(t)$. The horizontal edges moves vertically with velocity $2/\ell + (\alpha + \beta)/2$, while the vertical ones moves horizontally with velocity $H_g(\ell(t))$.

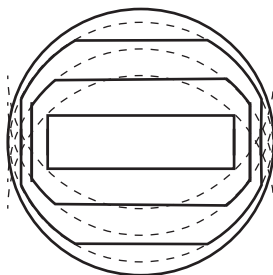


Figure 4.5. Effective evolution of a circle.

For example, the effective evolution starting from a circle is depicted in Figure 4.5.

References

- [1] F. ALMGREN and J. E. TAYLOR, *Flat flow is motion by crystalline curvature for curves with crystalline energies*, J. Differential Geom. **42** (1995), 1–22.
- [2] F. ALMGREN, J. E. TAYLOR and L. H. WANG, *Curvature-driven flows: a variational approach*, SIAM J. Control Optim. **31** (1993), 387–438.
- [3] L. AMBROSIO and A. BRAIDES, *Functionals defined on partitions of sets of finite perimeter, I: integral representation and Γ -convergence*, J. Math. Pures Appl. **69** (1990), 285–305.
- [4] L. AMBROSIO, N. GIGLI and G. SAVARÉ, “Gradient Flows in Metric Spaces and in the Space of Probability Measures”, Lectures in Mathematics ETH, Zürich. Birkhäuser, Basel, 2008.

- [5] G. BELLETTINI, R. GOGLIONE and M. NOVAGA, *Approximation to driven motion by crystalline curvature in two dimensions*, Adv. Math. Sci. Appl. **10** (2000), 467–493.
- [6] G. BELLETTINI, M. NOVAGA and M. PAOLINI, *Characterization of facet breaking for nonsmooth mean curvature flow in the convex case*, Interfaces Free Bound. **3** (2001), 415–446.
- [7] G. BELLETTINI, M. NOVAGA and M. PAOLINI, *On a crystalline variational problem, part I: first variation and global L^∞ regularity*, Arch. Ration. Mech. Anal. **157** (2001), 165–191.
- [8] G. BELLETTINI, M. NOVAGA and M. PAOLINI, *On a crystalline variational problem, part II: BV regularity and structure of minimizers on facets*, Arch. Ration. Mech. Anal. **157** (2001), 193–217.
- [9] A. BRAIDES, “ Γ -convergence for Beginners”, Oxford University Press, 2002.
- [10] A. BRAIDES, “Local Minimization, Variational Evolution and Γ -convergence”, Lecture Notes in Mathematics, Springer, Berlin, 2014.
- [11] A. BRAIDES, M. CICALESE and N. K. YIP, *Crystalline motion of interfaces between patterns*, J. Stat. Phys. **165** (2016), 274–319.
- [12] A. BRAIDES, M. COLOMBO, M. GOBBINO and M. SOLCI, *Minimizing movements along a sequence of functionals and curves of maximal slope*, C. R. Acad. Sci. Paris, Ser. I **354** (2016), 685–689.
- [13] A. BRAIDES, M. S. GELLI and M. NOVAGA, *Motion and pinning of discrete interfaces*, Arch. Ration. Mech. Anal. **95** (2010), 469–498.
- [14] A. BRAIDES and C. LARSEN, *Γ -convergence for stable states and local minimizers*, Ann. Sc. Norm. Sup. Pisa Cl. Sci. **10** (2011), 193–206.
- [15] A. BRAIDES and G. SCILLA, *Motion of discrete interfaces in periodic media*, Interfaces Free Bound. **15** (2013), 451–476.
- [16] A. BRAIDES and M. SOLCI, *Motion of discrete interfaces through mushy layers*, J. Nonlinear Sci. **26** (2016), 1031–1053.
- [17] A. CESARONI, N. DIRR and M. NOVAGA, *Homogenization of a semilinear heat equation*, J. Éc. Polytech. Math. **4** (2017), 633–660.
- [18] A. CESARONI, M. NOVAGA and E. VALDINOCI, *Curve shortening flow in heterogeneous media*, Interfaces Free Bound. **13** (2011), 485–505.
- [19] A. CHAMBOLLE and M. NOVAGA, *Approximation of the anisotropic mean curvature flow*, Math. Models Methods Appl. Sci. **17** (2007), 833–844.
- [20] M. COLOMBO and M. GOBBINO, *Passing to the limit in maximal slope curves: from a regularized Perona-Malik equation to the total variation flow*, Math. Models Methods Appl. Sci. **22** (2012), 1250017.
- [21] H. FEDERER, “Geometric Measure Theory”, Springer, Berlin, 1969.
- [22] A. F. FILIPPOV, “Differential Equations with Discontinuous Righthand Sides”, Vol. 18 of Mathematics and Its Applications. Dordrecht, The Netherlands, Kluwer Academic Publishers, 1988.
- [23] Y. GIGA, “Surface Evolution Equations. A Level set Approach”, Vol. 99 of Monographs in Mathematics. Birkhäuser Verlag, Basel, 2006.
- [24] M. H. GIGA, Y. GIGA and P. RYBKA, *A comparison principle for singular diffusion equations with spatially inhomogeneous driving force for graphs*, Arch. Ration. Mech. Anal. **211** (2014), 419–453.
- [25] Y. GIGA and M. E. GURTIN, *A comparison theorem for crystalline evolution in the plane*, Quart. Appl. Math. **54** (1996), 727–737.
- [26] Y. GIGA and P. RYBKA, *Facet bending in the driven crystalline curvature flow in the plane*, J. Geom. Anal. **18** (2008), 109–147.
- [27] Y. GIGA and P. RYBKA, *Facet bending driven by the planar crystalline curvature with a generic nonuniform forcing term*, J. Differential Equations **246** (2009), 2264–2303.
- [28] M. E. GURTIN, “Thermomechanics of Evolving Phase Boundaries in the Plane”, Oxford Mathematical Monographs, The Clarendon Press, Oxford University Press, New York, 1993.

- [29] A. MALUSA and M. NOVAGA, *Crystalline evolutions in chessboard-like microstructures*, Netw. Heterog. Media **13** (2010), 493–513.
- [30] A. MIELKE, *On evolutionary Γ -convergence for gradient systems*, In: “Macroscopic and Large Scale Phenomena: Coarse Graining, Mean Field Limits and Ergodicity”, Springer, Berlin, 2016, 187–249.
- [31] M. NOVAGA and E. VALDINOCI, *Closed curves of prescribed curvature and a pinning effect*, Netw. Heterog. Media **6** (2011), 77–88.
- [32] E. SANDIER and S. SERFATY, *Γ -convergence of gradient flows with applications to Ginzburg-Landau*, Comm. Pure Appl. Math. **57** (2004), 1627–1672.
- [33] J. E. TAYLOR, *Crystalline variational problems*, Bull. Amer. Math. Soc. **84** (1978), 568–588.

Dipartimento di Matematica
Università di Roma “Tor Vergata”
via della Ricerca scientifica
00133 Roma, Italia
braides@mat.uniroma2.it

Dipartimento di Matematica “G. Castelnuovo”
Sapienza Università di Roma
Piazzale Aldo Moro 2
00185 Roma, Italia
malusa@mat.uniroma1.it

Dipartimento di Matematica
Università di Pisa
Largo Pontecorvo 5
56217 Pisa, Italia
matteo.novaga@unipi.it